CCI+ PHASE 2
PERMAFROST

D5.1 CLIMATE ASSESSMENT REPORT (CAR)

VERSION 4.0

17 MAY 2024

PREPARED BY

Document status sheet

Issue	Date	Details	Authors
1.0	30.10.2019	first version, year 1	I. Nitze, G. Grosse, H. Matthes, M. Wieczorek, A. Bartsch, B. Heim
2.0	30.09.2020	second version: update of service case status and dissemination activities representing year 2	I. Nitze, G. Grosse, H. Matthes, M. Wieczorek, A. Bartsch, B. Heim
2.1	16.10.2020	Inclusion of IPA (represented through Isabelle Gärtner-Roer) evaluation	A. Bartsch
3.0	30.09.2021	update of service case status and dissemination activities representing year 3	I. Nitze, H. Matthes, M. Wieczorek, S. Lisovksi, B. Heim, A. Bartsch
3.1	19.01.2022	Update (name of cci dataset) in Table 1	A. Bartsch
4.0	17.05.2024	update of service case status and dissemination activities representing year 4 (CCI phase II); inclusion of rock glacier monitoring	I. Nitze, G. Grosse, H. Matthes, M. Wieczorek, B. Heim, A . Bartsch, L. Rouyet, T. Echelard, L. Schmid, C. Pellet, R. Delaloye, F. Sirbu, A. Omacu, V. Poncos, F. Brardinoni, A. Kääb, T. Strozzi, N. Jones

Author team

Guido Grosse, Ingmar Nitze, Birgit Heim, Mareike Wieczorek, Heidrun Matthes, AWI
Line Rouyet, Thomas Echelard, Lea Schmid, Cécile Pellet, Reynald Delaloye, UNIFR
Flavius Sirbu, Alexandru Onaca, WUT
Valentin Poncos, Terrasigna
Francesco Brardinoni, University of Bologna
Line Rouyet, NORCE
Andreas M. Kääb, UiO
Tazio Strozzi and Nina Jones, GAMMA
Annett Bartsch, BGEOS

ESA Technical Officer

Frank Martin Seifert

TABLE OF CONTENTS

Executive summary

This document presents the Climate Assessment Report (CAR) version 4 of the European Space Agency (ESA) Climate Change Initiative (CCI) Permafrost project (Permafrost_cci). CCI is ESA's global monitoring program whose main objective is to provide Earth Observation (EO)-based Essential Climate Variable (ECV) timeseries to the climate modelling and climate user communities. There is currently no consistent global Earth Observation-based mapping of the parameters permafrost temperature and active layer thickness as required by GCOS based on Earth Observation records. Permafrost_cci will for the first time provide such information for different epochs and meet the requirements for the production of a climate data record. Permafrost_cci was part of phase I of CCI+ (2018–2021) and has been selected for phase II (2022–2025) with the production of ECVs for permafrost, set by the Global Climate Observing System (GCOS)/World Meteorological Organisation (WMO). The CAR describes the scientific assessments of the produced variables for the ECV: : i) permafrost temperature expressed as Ground Temperature per Depth (GTD) [°C] ii) Active Layer Thickness (ALT) [cm], iii) permafrost extent expressed as Permafrost Fraction (PFR) [%] derived from GTD at 2 m depth, iv) Rock Glacier Inventory (RoGI) and, v) and Rock Glacier Velocity (RGV). The CAR also summarizes the Use Cases of the Permafrost_cci products and current activities within Permafrost_cci with regard to user requirements defined by the climate modelling user community.

Use case #1 summarises usage of the CCI Permafrost product in conjunction with the Land Surface Model (LSM) Community Land Model 5 (CLM5). Permafrost dynamics representations of CLM5 were compared to CCI Permafrost derived mean annual ground temperature (MAGT) and permafrost extent (PF) in order to evaluate the model performance and potential model improvement through sensitivity studies. A spatial comparison of the climatological mean of MAGT between model and observation was conducted to assess the model performance in different regions.

For use case #2, a comparison of Landsat derived trends separated between fire and non-fire affected areas has been added in this version. Particularly increasing variance within burned areas, with locally strong increase in ALT, may result in triggering further permafrost disturbances. However, more detailed analysis will be conducted to verify/falsify this hypothesis.

A third use case #3 covers a joint study with H2020 Nunataryuk which had a focus on infrastructure across the Arctic. Almost 97% of all mapped objects showed a positive trend in ground temperature and 93% for ALT (CRDPv2). 55% of the identified human impacted area will be shifting to above 0 ◦C ground temperature at two meter depth by 2050 if current permafrost warming trends continue at the pace of the last two decades.

Based in result of the PVIR, Permafrost_cci GTD and PFR products for the Northern hemisphere are considered to be most reliable in the permafrost temperature range with GTD < 1°C and in PFR >50% as well as PFR <14% is reliable as non-permafrost.

Recommendations from the user workshops held at the European Permafrost Conference EUCOP 2023 in Puigcerda, Spain, including the WMO GTN-P general assembly meeting, included an increased temporal as well as vertical resolution of the CryoGrid products, specifically to facilitate climate modelling applications requiring these resolutions.

Use case #4 evaluates the value of using spaceborne Interferometric Synthetic Aperture Radar (InSAR) based on Sentinel-1 SAR and ALOS-2 PALSAR-2 images, to assign a kinematic attribute to the inventoried landforms and improve the assessment of rock glacier activity. The results show the value of InSAR for the systematic documentation of the rock glacier creep rate at the regional scale. The use case also highlighted several limitations in the Rock Glacier Inventory (RoGI) procedure applied in Permafrost_cci Phase 1. The conclusions contributed to update the workflow for RoGI production in Permafrost_cci Phase 2.

The preliminary assessment of the Permafrost_cci RGV products show that the InSAR-RGV result from the iteration 1 Permafrost_cci Phase 2 are promising. We propose an easily transferable method to automate the production of RGV by averaging unwrapped Sentinel-1 interferograms. The developed method appears to be suitable to produce consistent InSAR-RGV, which are comparable to GNSS-RGV, although we need to include more years of data to confirm this primary conclusion.

1 Introduction

1.1 Purpose of the document

This document is the Climate Assessment Report (CAR) version 4 (update of [RD-1]) of the ESA CCI+ project Permafrost_cci providing the user requirements of climate science and climate services for Permafrost_cci ECV products, the Climate Research Data Packages (CRDP) of the Permafrost_cci project. Besides the required WMO/GCOS Permafrost ECVs i) permafrost temperature, and ii) active layer thickness, Permafrost_cci provides iii) permafrost extent (permafrost fraction within a pixel), as an additional variable derived from permafrost temperature: the areal fraction within the grid cell that fulfills the definition for the existence of permafrost (ground temperature <0 ºC for two consecutive years), , iv) Rock Glacier Inventory (RoGI) and, v) and Rock Glacier Velocity (RGV).

The generation of the Permafrost_cci CRDP i) Ground Temperature per Depth (GTD) per year, Active Layer Thickness (ALT) per year, and Permafrost FRaction (PFR) per year time series relies on the ground thermal model Permafrost_cci CryoGrid, that is forced by EO time series of Land Surface Temperature (LST) and Snow Water Equivalent (SWE) with boundary conditions of EO-derived Land Cover [RD-3].

The Permafrost_cci CRDPv3 [RD-3] released in 2023, is an update of CRDPv2 and includes three time series covering the Northern Hemisphere north of 30° N:

- simulated EO-forced **mean annual Ground Temperature per Depth (GTD) in five discrete depths** (0 m, 1 m, 2 m, 5 m, 10 m) from 1997 to 2021
- simulated EO-forced **annual Active Layer Thickness (ALT)** from 1997 to 2021
- **annual Permafrost FRaction (PFR)** derived from GTD from 1997 to 2021

Rock glacier product include:

- Inventories (RGI) in selected regions
- Rock glacier velocity time series of annualised surface velocity values expressed in m/y and measured/computed on a rock glacier or a part of it.

1.2 Structure of the document

The CAR is organized in 6 chapters. Chapter 1 provides the introduction and the overview on Permafrost_cci including applicable documents and the community glossary for Permafrost. Chapter 2 summarized the products of Permafrost_cci. Chapter 3 and its subsections describe the use cases and assessment. Further progress is documented in chapter 4, what also includes plans for operationalization. Chapter 5 lists publications and outreach, Chapter 6 the references.

1.3 Applicable documents

[AD-1] GEO/CEOS Quality Assurance framework for Earth Observation (QA4EO) protocols 3-4

[AD-2] ESA 2017: Climate Change Initiative Extension (CCI+) Phase 1 – New Essential Climate Variables – Statement of Work. ESA-CCI-PRGM-EOPS-SW-17-0032

[AD-3] ESA Climate Change Initiative. CCI Project Guidelines. EOP-DTEX-EOPS-SW-10-0002

[AD-4] ECV 9 Permafrost: Assessment report on available methodological standards and guides, 1 Nov 2009, GTOS-62

[AD-5] Requirements for monitoring of permafrost in polar regions - A community white paper in response to the WMO Polar Space Task Group (PSTG), Version 4, 2014-10-09. Austrian Polar Research Institute, Vienna, Austria, 20 pp.

[AD-6] ESA. 2022. Climate Change Initiative Extension (CCI+) Phase 2 – New Essential Climate Variables – Statement of Work. ESA-EOP-SC-AMT-2021-27.

[AD-7] GCOS. 2022. The 2022 GCOS Implementation Plan. GCOS – 244 / GOOS – 272. Global Observing Climate System (GCOS). World Meteorological Organization (WMO).

[AD-8] GCOS. 2022. The 2022 GCOS ECVs Requirements. GCOS – 245. Global Climate Observing System (GCOS). World Meteorological Organization (WMO).

[AD-9] GTN-P. 2021. Strategy and Implementation Plan 2021–2024 for the Global Terrestrial Network for Permafrost (GTN-P). Authors: Streletskiy, D., Noetzli, J., Smith, S.L., Vieira, G., Schoeneich, P., Hrbacek, F., Irrgang, A.M.

1.4 Reference Documents

[RD-1] Nitze, I., Grosse, G., Heim, B., Wieczorek, M., Matthes, H., Bartsch, A., Strozzi, T. (2019): ESA CCI+ Climate Assessment Report, v1.0

[RD-2] Nitze, I., Grosse, G., Heim, B., Wieczorek, M., Matthes, H., Bartsch, A., Strozzi, T. (2020): ESA CCI+ Climate Assessment Report, v2.0

[RD-3] Nitze, I., Grosse, G., Heim, B., Wieczorek, M., Matthes, H., S. Lisovski Bartsch, A., Strozzi, T. (2021): ESA CCI+ Climate Assessment Report, v3.0

[RD-4] van Everdingen, Robert, ed. 1998 revised May 2005. Multi-language glossary of permafrost and related ground-ice terms. Boulder, CO: National Snow and Ice Data Center/World Data Center for Glaciology. (http://nsidc.org/fgdc/glossary/; accessed 23.09.2009)

[RD-5] Bartsch, A., Westermann, Strozzi, T., Wiesmann, A., Kroisleitner, C., 2019: ESA CCI+ Permafrost Product Specifications Document, v1.0

[RD-6] Bartsch, A., Westermann, Strozzi, T., Wiesmann, A., Kroisleitner, C., 2021: ESA CCI+ Permafrost Product Specifications Document, v2.0

[RD-7] Rouyet, L., Pellet, C., Delaloye, R., Onaca, A., Sirbu, F., Poncos, V., Brardinoni, F., Kääb, A., Strozzi, T., Jones, N., Bartsch, A. 2023. ESA CCI+ Permafrost Phase 2 – CCN4 Mountain Permafrost: Rock Glacier Inventories (RoGI) and Rock glacier Velocity (RGV) Products. D1.1 User Requirement Document (URD), v1.0. European Space Agency.

[RD-8] Rouyet, L., Pellet, C., Delaloye, R., Onaca, A., Sirbu, F., Poncos, V., Brardinoni, F., Kääb, A., Strozzi, T., Jones, N., Bartsch, A. 2023. ESA CCI+ Permafrost Phase 2 – CCN4 Mountain Permafrost: Rock Glacier Inventories (RoGI) and Rock glacier Velocity (RGV) Products. D1.2 Product Specification Document (PSD), v1.0. European Space Agency.

[RD-9] RGIK, 2023. Puigcerdà Commitment. IPA Action Group Rock glacier inventories and kinematics, 4 pp.

[RD-10] Rouyet, L., Echelard, T., Schmid, L., Pellet, C., Delaloye, R., Onaca, A., Sirbu, F., Poncos, V., Brardinoni, F., Kääb, A., Strozzi, T., Jones, N., Bartsch, A. 2023. ESA CCI+ Permafrost Phase 2 – CCN4 Mountain Permafrost: Rock Glacier Inventories (RoGI) and Rock glacier Velocity (RGV) Products. D3.2 Climate Research data Package (CRDP), v1.0. European Space Agency.

[RD-11] Rouyet, L., Echelard, T., Schmid, L., Pellet, C., Delaloye, R., Onaca, A., Sirbu, F., Poncos, V., Brardinoni, F., Kääb, A., Strozzi, T., Bartsch, A. 2024. ESA CCI+ Permafrost Phase 2 – CCN4 Mountain Permafrost: Rock Glacier Inventories (RoGI) and Rock glacier Velocity (RGV) Products. D4.1 Product Validation and Intercomparison Report (PVIR), v1.0. European Space Agency.

[RD-12] Rouyet, L., Echelard, T., Schmid, L., Pellet, C., Delaloye, R., Onaca, A., Sirbu, F., Poncos, V., Brardinoni, F., Kääb, A., Strozzi, T., Bartsch, A. 2024. ESA CCI+ Permafrost Phase 2 – CCN4 Mountain Permafrost: Rock Glacier Inventories (RoGI) and Rock glacier Velocity (RGV) Products. D4.2 Product User Guide (PUG), v1.0. European Space Agency.

[RD-13] Bertone, A., Barboux, C., Delaloye, R., C., Rouyet, L., Lauknes, T.R., Kääb, A., Christiansen, H.H., Onaca, A., Sirbu, F., Poncos, V., Strozzi, T., Caduff, R., Bartsch, A. 2020. ESA CCI+ Permafrost Phase I – CCN1 & CCN2 Mountain Permafrost: Rock Glacier Kinematics as New Associated Parameter of ECV Permafrost. D4.2 Climate Research data Package (CRDP), v1.0. European Space Agency.

[RD-14] Rouyet, L., Lauknes, T.R., Barboux, C., Bertone, A., Delaloye, R., C., Kääb, A., Christiansen, H.H., Onaca, A., Sirbu, F., Poncos, V., Strozzi, T., Caduff, R., Bartsch, A. 2020. ESA CCI+ Permafrost Phase I – CCN1 & CCN2 Mountain Permafrost: Rock Glacier Kinematics as New Associated Parameter of ECV Permafrost. D2.2 Algorithm Theoretical Basis Document (ATBD), v1.0. European Space Agency.

1.5 Bibliography

A complete bibliographic list that supports arguments or statements made within the current document is provided in Section 6.1.

1.6 Acronyms

A list of acronyms is provided in section 6.2.

1.7 Glossary

The glossary below based on [RD-4] and [AD-2] provides a selection of terms relevant for the Climate Change Initiative. A comprehensive glossary is available as part of the Product Specifications Document [RD-4,5,8].

active-layer thickness

The thickness of the ground layer that is subject to annual thawing and freezing above permafrost. The thickness of the active layer depends on factors such as the ambient air temperature, vegetation, drainage, soil or rock type and total water content, snowcover, and degree and orientation of slope. As a rule, the active layer is thin in the High Arctic (it can be less than 15 cm) and becomes thicker farther south (1 m or more). The thickness of the active layer can vary from year to year, primarily due to variations in the mean annual air temperature, distribution of soil moisture, and snowcover. The thickness of the active layer includes the uppermost part of the permafrost wherever either the salinity or clay content of the permafrost allows it to thaw and refreeze annually, even though the material remains cryotic (T <0 °C).

Use of the term "depth to permafrost" as a synonym for the thickness of the active layer is misleading, especially in areas where the active layer is separated from the permafrost by a residual thaw layer, that is, by a thawed or noncryotic (T >0 °C) layer of ground.

REFERENCES: Muller, 1943; Williams, 1965; van Everdingen, 1985

continuous permafrost

Permafrost occurring everywhere beneath the exposed land surface throughout a geographic region with the exception of widely scattered sites, such as newly deposited unconsolidated sediments, where the climate has just begun to impose its influence on the thermal regime of the ground, causing the development of continuous permafrost. For practical purposes, the existence of small taliks within continuous permafrost has to be recognized. The term, therefore, generally refers to areas where more than 90 percent of the ground surface is underlain by permafrost.

REFERENCE: Brown, 1970.

discontinuous permafrost

Permafrost occurring in some areas beneath the exposed land surface throughout a geographic region where other areas are free of permafrost. Discontinuous permafrost occurs between the continuous permafrost zone and the southern latitudinal limit of permafrost in lowlands. Depending on the scale of mapping, several subzones can often be distinguished, based on the percentage (or fraction) of the land surface underlain by permafrost, as shown in the following table.

Permafrost	English usage	Russian Usage
Extensive	65-90%	Massive Island
Intermediate	35-65%	Island
Sporadic	10-35%	Sporadic
Isolated Patches	0-10%	-

SYNONYMS: (not recommended) insular permafrost; island permafrost; scattered permafrost.

REFERENCES: Brown, 1970; Kudryavtsev, 1978; Heginbottom, 1984; Heginbottom and Radburn, 1992; Brown et al., 1997.

mean annual ground temperature (MAGT)

Mean annual temperature of the ground at a particular depth. The mean annual temperature of the ground usually increases with depth below the surface. In some northern areas, however, it is not uncommon to find that the mean annual ground temperature decreases in the upper 50 to 100 metres below the ground surface as a result of past changes in surface and climate conditions. Below that depth, it will increase as a result of the geothermal heat flux from the interior of the earth. The mean annual ground temperature at the depth of zero annual amplitude is often used to assess the thermal regime of the ground at various locations.

permafrost

Ground (soil or rock and included ice and organic material) that remains at or below 0 °C for at least two consecutive years. Permafrost is synonymous with perennially cryotic ground: it is defined on the basis of temperature. It is not necessarily frozen, because the freezing point of the included water may be depressed several degrees below 0°C; moisture in the form of water or ice may or may not be present. In other words, whereas all perennially frozen ground is permafrost, not all permafrost is perennially frozen. Permafrost should not be regarded as permanent, because natural or man-made changes in the climate or terrain may cause the temperature of the ground to rise above 0 °C. Permafrost includes perennial ground ice, but not glacier ice or icings, or bodies of surface water with temperatures perennially below 0 °C; it does include man-made perennially frozen ground around or below chilled pipe-lines, hockey arenas, etc.

Russian usage requires the continuous existence of temperatures below 0 °C for at least three years, and also the presence of at least some ice.

SYNONYMS: perennially frozen ground, perennially cryotic ground and (not recommended) biennially frozen ground, climafrost, cryic layer, permanently frozen ground.

REFERENCES: Muller, 1943; van Everdingen, 1976; Kudryavtsev, 1978.

Rock glacier (RoGI)

Debris landforms generated by the former or current creep of frozen ground (permafrost), detectable in the landscape with the following morphologies: front, lateral margins and optionally ridge-and-furrows surface topography. Reference: RGIK. 2023. Guidelines for inventorying rock glaciers: baseline and practical concepts (version 1.0). IPA Action Group Rock Glacier Inventories and Kinematics, 25 pp. DOI: 10.51363/unifr.srr.2023.002.

Rock glacier velocity (RGV)

Time series of annualised surface velocity values expressed in m/y and measured/computed on a rock glacier or a part of it. Reference: RGIK. 2023. Rock glacier velocity as an associated parameter of ECV Permafrost: Baseline concepts (version 3.2). IPA Action Group Rock Glacier Inventories and Kinematics, 12 pp.

2 Products generated by Permafrost_cci

Permafrost_cci baseline component is establishing Earth Observation (EO) based products for the permafrost ECV spanning the period from 1997 to 2021. The required Permafrost ECVs by WMO/GCOS for Permafrost are [AD-2,3,4] i) **permafrost temperature** and ii) **active layer thickness**. Permafrost_cci added iii) **permafrost extent** (permafrost fraction) as a mapped permafrost variable, which is the fraction within an area (pixel) for which the definition for the existence of permafrost (ground temperature < 0 ºC for two consecutive years) is fulfilled. The main focus of Permafrost_cci lies on the ECV permafrost temperature, as its derivation also forms the base for the producing the active layer thickness and permafrost fraction variables.
Since ground temperature and seasonal thaw depth cannot be directly observed with space-borne sensors, a variety of satellite and reanalysis data are combined in a ground thermal model to infer these subsurface parameters. The algorithm uses remotely sensed data sets of Land Surface Temperature (MODIS LST/ ESA LST CCI) and landcover (ESA Landcover CCI) to drive the transient permafrost model CryoGrid-3 (CryoGrid-2 in Obu et al., 2019), which yields thaw depth and ground temperature at various depths, while ground temperature then forms the basis for deriving permafrost fraction for a specified location and time.

The Permafrost Climate Research Data Package (CRDP v2) Version 3.0 of the Climate Research Data Package [RD-3] consists of time series covering the years from 1997 and 2021 for

i) Permafrost temperature expressed as Ground Temperature per Depth (GTD) [°C]

ii) Active Layer Thickness (ALT) [cm] (maximum annual active layer depth)

iii) Permafrost extent expressed as Permafrost FRaction (PFR) [%] derived from GTD at 2 m depth.

The **mountain permafrost component** of Permafrost_cci Phase 2 focuses on the generation of two products: **Rock Glacier Inventory** (RoGI) and **Rock Glacier Velocity** (RGV) [AD-5]. The user relevance and rationale to define the product specifications have been described in the URD [RD-8] and PSD [RD-9].

In periglacial mountain environments, the permafrost occurrence is patchy and the preservation of permafrost is controlled by site-specific conditions, which require the development of dedicated products as a complement to GT and ALT measurements and permafrost models. Rock glaciers are the best visual expression of the creep of mountain permafrost and constitute an essential geomorphological heritage of the mountain periglacial landscape. Their dynamics is largely influenced by climatic factors. There are increasing evidence that the interannual variations of the rock glacier creep rates are influenced by changing permafrost temperature, making RGV a key parameter for the monitoring of the cryosphere in mountains.

The integration of RoGI and RGV products in Permafrost_cci Phase 2 agrees with the objectives of the *Rock Glacier Inventories and Kinematics* (RGIK) community [RD-9]. RoGI is a valuable product to document past and present permafrost extent in mountains. It is a recommended first step to comprehensively characterise and select the landforms that can be used for RGV monitoring. The systematic generation of an international RGV database concurs with the recent GCOS and GTN-P decisions to add RGV as a new product of the ECV Permafrost to monitor changing mountain permafrost conditions [AD-6 to AD-8].

RoGI and RGV products form a unique validation dataset for climate models in mountain regions, where direct permafrost measurements are very scarce or even totally lacking. Using satellite remote sensing, generating systemic RoGI at the regional scale and documenting RGV interannual changes over many landforms become feasible. Within Permafrost_cci, we mostly use Synthetic Aperture Radar Interferometry (InSAR) technology based on Sentinel-1 images that provide a global coverage, a large range of detection capability (mm–cm/yr to m/yr) and fine spatio-temporal resolutions (tens of m pixel size and 6–12 days of repeat-pass). InSAR can be complemented by SAR offset tracking technique and spaceborne/airborne optical photogrammetry.

3 Assessment of products and other feedback

3.1 Introduction and rationale

Warming of the Cryosphere is already exceeding the global average temperature increase and models project further strong warming for these regions (IPCC 2021, IPCC, 2019; IPCC, 2013). Permafrost is an important component of the Cryosphere and defined as ground that remains frozen for at least two consecutive years (Van Everdingen, 1998). Ongoing permafrost warming (Romanovsky et al., 2010; Biskaborn et al., 2019) and near-surface thawing in permafrost regions, associated with rising air temperatures, are considered to reinforce warming of the atmosphere through the partial conversion of the large permafrost soil organic carbon pool into greenhouse gases, a process termed "permafrost carbon feedback" (Schuur et al., 2015). A further challenge for monitoring the impacts of permafrost thaw dynamics is represented by rapid thaw processes that may mobilize a significant amount of carbon over short time spans of years to decades (Turetsky et al., 2019). Worldwide monitoring of permafrost is therefore essential to understand and assess the feedbacks between climate change and permafrost thaw and their impact on the Earth's climate system.

The recently published thorough analysis of global permafrost temperatures by the Global Terrestrial Network for Permafrost (GTN-P) and the International Permafrost Association (IPA) demonstrated that permafrost is warming at a global scale (Biskaborn et al., 2019). This study showed that during the reference decade (2007 to 2016) ground temperature near the depth of zero annual amplitude in the continuous permafrost zone increased by 0.39 ± 0.15 °C. Over the same period, discontinuous permafrost warmed by 0.20 ± 0.10 °C. Permafrost in mountains warmed by 0.19 ± 0.05 °C and in Antarctica by 0.37 ± 0.10 °C. Globally, permafrost temperature increased by 0.29 ± 0.12 °C.

However, despite the great efforts by the GTN-P/IPA in managing qualified long-term permafrost observations at a global scale, the observation points are very scarce and clustered. For example, Biskaborn et al. (2015) pointed out that GTN-P permafrost boreholes and active layer measurement sites are clustered along transportation corridors in areas with developed infrastructure. They further demonstrated that the distribution of GTN-P sites is concentrated within zones where projected temperature rise is smaller while a much lower number of sites are located within Arctic areas where climate models project very large temperature increases.

There is currently no globally consistent and spatially continuous mapping of the ECV parameters permafrost temperature and active layer thickness. IPA had therefore established a permafrost mapping focus group (action group 'Overseeing the production of the next generation of IPA global permafrost mapping product and service'), which seeked to assess different permafrost mapping initiatives for the compilation of a new global database for permafrost properties. Permafrost_cci contributes to this IPA activity by providing satellite-driven permafrost datasets. The Permafrost_cci products are further expected to aid understanding of permafrost dynamics by satellite-observed land surface changes across large regions, in particular disturbances along latitudinal gradients as well as degradation associated with permafrost coastal processes.

The following sections provide a first assessment of the CRDPv0, v1, v2, and v3 by the climate research group with respect to the so far identified applications.

Three Use Case studies cover a broad range of applications demonstrating the value and impact of CCI+ Permafrost products for different aspects of climate research. A utility assessment based on the PVIR is provided in addition.

3.2 Use Case Study 1 - Climate modelling: Evaluating permafrost dynamics representation in a land surface model

Key points:

- Permafrost dynamics representations of the Land Surface Model CLM5 are compared to CCI Permafrost derived mean annual ground temperature (MAGT) and permafrost extent (PF) in order to evaluate the model performance and potential model improvement through sensitivity studies.
- We perform a spatial comparison of the climatological mean of MAGT between model and observation to assess the model performance in different regions. PF is compared in a binary mode.
- Both sensitivity studies show improvements over the performance of the standard model setup. The changes in snow thermal conductivity we propose are going to become a standard option for running CLM5.

Service:

- Model development
- Permafrost degradation and permafrost carbon feedback assessment
- Adaptation

End user (s)

- CMIP7 Model developers
- Researchers

Intermediate user (s)

- Research institutes and academia, many Land Surface Models show similar biases in their permafrost dynamics representation as CLM5, so our results can help improve many models

Applications

Approximately 11% of the world's exposed land contains permafrost, predominantly in regions experiencing rapid climate change. Over the last decade, permafrost temperatures have generally increased in the circum-Arctic, leading to notable shifts in hydrology, landscapes, biogeochemical cycles, ecosystems, biodiversity, infrastructure, and overall sustainability of life on permafrost. In addition, Arctic and subarctic soils contain a vast carbon reservoir, estimated to be about twice the amount in the Earth's atmosphere. Most of this carbon is currently locked in permafrost, but global warming is making this organic matter more prone to decomposition. This, in turn, contributes to rising CO2 and CH4 emissions, thus underlining the significance of permafrost carbon feedback in the climate system. In order to understand the impacts of these feedbacks and changes under future climate projections, land surface models need to accurately represent permafrost dynamics, which makes the development and evaluation of these models crucial for the upcoming CMIP7.

Essential Climate Variables

- Cryosphere
    - Permafrost ground temperature

- Permafrost Extent

Models

- Community Land Model version 5 (Lawrence et al., 2019)

Climate Data Records

ESA Permafrost Climate Change Initiative (Permafrost_cci): Permafrost version 2 data products, Obu, J.; Westermann, S.; Barboux, C.; Bartsch, A.; Delaloye, R.; Grosse, G.; Heim, B.; Hugelius, G.; Irrgang, A.; Kääb, A.M.; Kroisleitner, C.; Matthes, H.; Nitze, I.; Pellet, C.; Seifert, F.M.; Strozzi, T.; Wegmüller, U.; Wieczorek, M.; Wiesmann, A. (2020): ESA Permafrost Climate Change Initiative (Permafrost_cci): Permafrost version 2 data products. Centre for Environmental Data Analysis, *15.05.2024*.. http://catalogue.ceda.ac.uk/uuid/1f88068e86304b0fbd34456115b6606f

Agencies

- European Space Agency (ESA) Climate Change Initiative (CCI)

Satellite observations

- MODIS Landsurface temperature

Description

Land Surface representation in ESMs has advanced significantly over the past decades, with process representation evolving from the basic surface energy fluxes to explicit consideration of dynamic vegetation, carbon cycling, crops or urban areas and very recently even considering lateral interaction between grid cells and between landscape units. Within these developments, physical processes necessary to represent permafrost dynamics within sophisticated Land Surface Models have been included. Coupled Earth System Models make use of these developments through incorporation of sophisticated Land Surface Models. Within these coupled models, permafrost dynamics representation depends on physical descriptions of soil processes and soil-snow-vegetation interactions. Using spatial data sets for evaluation of permafrost representation is essential to accurately asses model capabilities with regards to permafrost.

Here, we use the state-of-the art land surface model CLM5 (Lawrence et al., 2019) to simulate present day permafrost conditions. The model was forced by ERA5 reanalysis data from 2000-2020. In the simulation using the standard configuration of CLM5 (control), we identified a significant cold bias in soil temperatures (see Figure 1a). The comparison of simulated MAGT at 1m depth shows a much colder control run especially over Siberia, where temperature differences are up to -8K. Over the Alaskan region, the model is much closer to ESA-CCI, with some areas still showing a difference around -2K. Some positive bias is observed over mountainous regions, such as the north coast of Baffin Island. However, this is likely attributed to the difference in resolution of the two products. ESA-CCI derives its forcings from daily ERA5 reanalysis data and are downscaled using the 1 km Global Multi-resolution Terrain Elevation Data (Westermann et al., 2020). Using this process, ESA-CCI uses atmospheric forcings on a much finer resolution (1 km^2) than the atmospheric forcings utilized in the simulation (12km^2). This difference in resolution allows ESA-CCI to more accurately represent cold high-elevation areas, explaining the observed warm bias. There is strong agreement between the CLM5 and ESA CCI+

Permafrost calculated permafrost extents, with 93% of the two datasets overlapping, including the discontinuous Arctic permafrost regions (Figure 2a), with a total extent of 13.358 and 12.544 ×106 km2 for CLM5 and ESA CCI+ Permafrost, respectively. However, there is a slight overestimation of permafrost extent in the CLM5 results in the southern regions of Alaska, Canada, and particularly Siberia.

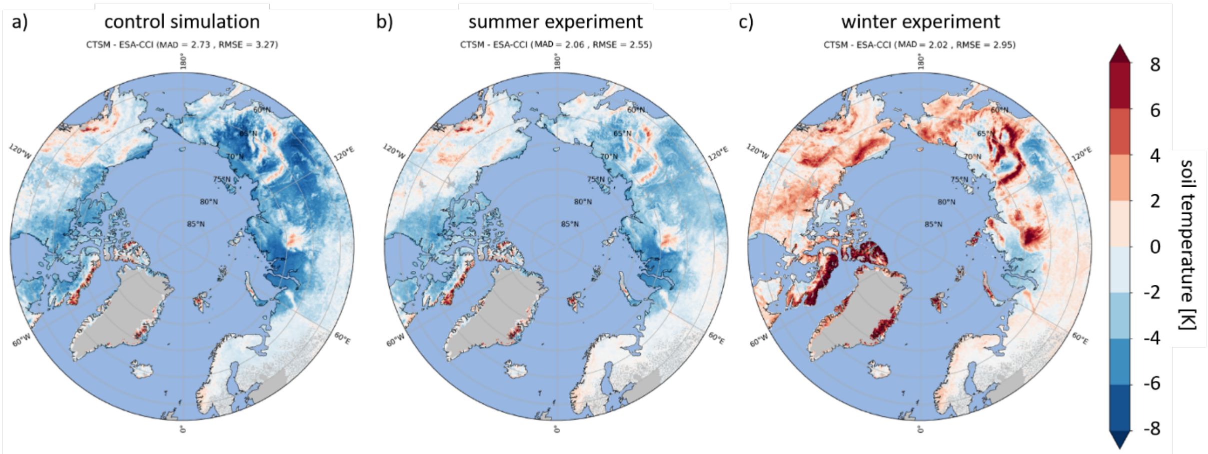

Figure 1: Comparisons of simulated MAGT at 1m depth with CCI+ Permafrost for the control simulation, the summer and the winter experiment.

In order to address the observed bias, we employed too different sensitivity studies: 1) modification of snow thermal conductivity using suggestions from Dutch et al. (2022) (winter experiment) and 2) modification of soil texture and organic matter content according to the CCI+ Permafrost Stratigraphy product (summer experiment). Figure 1b compiles an evaluation of the MAGT at 1m depth versus ESA CCI+ Permafrost. The summer experiment has effectively mitigated a part of the cold bias observed in the control run. While the spatial heterogeneity of the bias stays identical, we observed a reduction in the cold bias of up to 4K This decrease is greater over areas like Siberia where the cold bias is strong in the control run. Only the Ural region show a bias above -4K. The warm bias observed over high-altitude regions is still present. The MAD and RMSE show a strong improvement, decreasing from 2.73 in the control run to 2.06 in the summer experiment, and from 3.27 to 2.55, respectively. In general, the summer experiment demonstrates a closer alignment to ESA CCI+ permafrost in terms of permafrost extent compared to the control simulation, with the total permafrost area measuring 12.857 ×106 km^2, compared to 12.544 ×106 km^2 for ESA CCI+ Permafrost (Figure 2b). Significant changes are observed in the southern region of Canada, where all permafrost areas simulated by CLM5 but not captured in ESA CCI+ Permafrost have been eliminated. Additionally, the extensive permafrost area in the Southwestern Europe, previously absent in ESA-CCI, experienced a substantial reduction. Despite the improvements, disparities between ESA-CCI and the model persist, particularly in northern Greenland, western Alaska, and southern regions of western Siberia and Europe. These findings indicate that the summer experiment successfully enhances the model's representation of permafrost extent, aligning it more closely with ESA CCI+ Permafrost, although some discrepancies still exist in specific geographic regions.

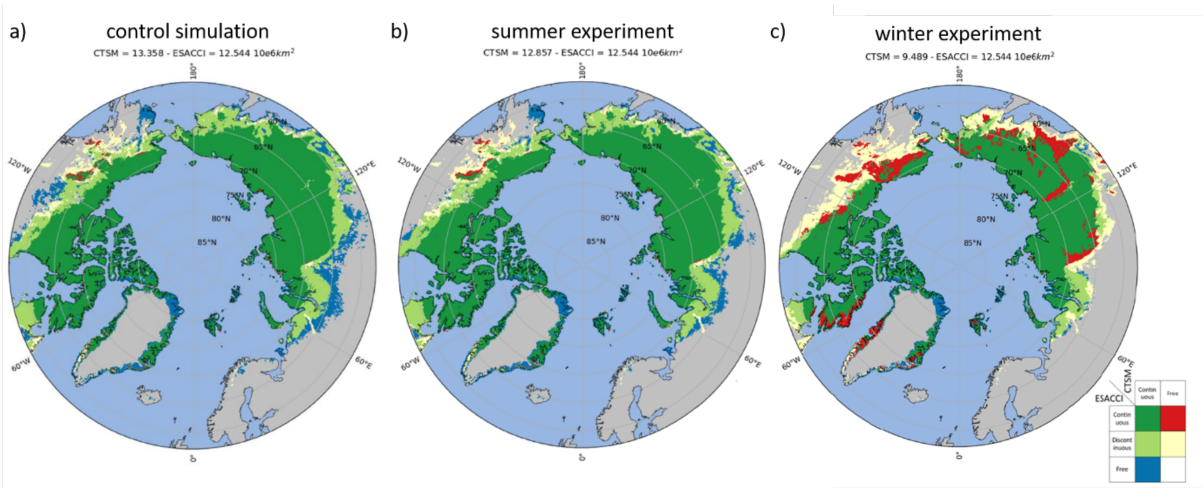

Figure 2: Comparisons of simulated permafrost extent with CCI+ Permafrost for the control simulation, the summer and the winter experiment.

It is evident that the winter experiment effectively mitigated a significant portion of the cold bias observed in the control run (Figure 1c). Most regions only have a small cold bias, typically reaching up to -2K. The MAD shows a noteworthy improvement, decreasing from 2.73 in the control run to 2.02 in the Sturm run. However, the spread of temperature values, represented by the RMSE, only reduced slightly, from 3.27 to 2.95. This is probably linked the pronounced warm bias observed over high-altitude areas, a feature that was present in the control run but was significantly amplified in the winter experiment. These high altitude regions encompass the central Siberian Plateau, the Verkhoyansk Range, most of Eastern Siberia, the northern regions of Baffin Island, and the Brooks Range. The overestimation of permafrost observed from the control run has been resolved to the detriment of mountainous regions (Figure 2c, in red) that have been reclassified as non-permafrost by the winter experiment. In addition, the winter experiment shows a significant loss of discontinuous permafrost (in yellow). This induces a significant decrease of 9.489 ×106 km2, compared to 12.544 ×106 km2 for ESA CCI+ Permafrost.
Both sensitivity experiments demonstrate that considerable improvements in model performance can be achieved through parameter modifications.

3.3 Use Case Study 2 -ALT, PFR and ground temperature trends: comparison to landcover trends

Key points:

- The HRPC (Hot Spot Regions of Permafrost Change) dataset, including lake changes and wildfires, was compared with The ESA CCI Ground Temperature dataset, and further auxiliary datasets of elevation, permafrost properties and thermokarst landscapes.
- State-of-the art explainable AI SHAP values were calculated to determine key environmental drivers of lake change over 600,000 lakes across the Arctic. in a second analysis the impact of wildfires was calculated for post-wildfire areas.
- The likelihood of lake drainage in permafrost regions is primarily influenced by the lake's origin and local lake morphologies, with the main factors varying across different regions. Notably,

peak drainage occurs in "warm" permafrost, characterized by a mean annual ground temperature ranging from -8 to -3 °C.

Service:

- Adaptation
- Planning

End user (s)

- Modellers
- Local communities
- Policy makers
- Government agencies
- Researchers

Intermediate user (s)

- Research institutes and academia

Applications

Permafrost is changing significantly due to the rapidly changing climate. Permafrost landscapes are changing rapidly with potentially strong impacts on local biogeochemical cycles but also implications on the global climate. Over the past years first pan-Arctic landscape disturbance maps and datasets have been created and published. These datasets can be used to better quantify environmental drivers of landscape change. With this information, it will become possible to project future landscape dynamics of a further warming arctic.

Essential Climate Variables

- Cryosphere
    - Permafrost ground temperature
    - Active Layer Thickness

Climate Data Records

ESA Permafrost Climate Change Initiative (Permafrost_cci): Permafrost version 2 data products, Obu, J.; Westermann, S.; Barboux, C.; Bartsch, A.; Delaloye, R.; Grosse, G.; Heim, B.; Hugelius, G.; Irrgang, A.; Kääb, A.M.; Kroisleitner, C.; Matthes, H.; Nitze, I.; Pellet, C.; Seifert, F.M.; Strozzi, T.; Wegmüller, U.; Wieczorek, M.; Wiesmann, A. (2020): ESA Permafrost Climate Change Initiative (Permafrost_cci): Permafrost version 2 data products. Centre for Environmental Data Analysis, *15.05.2024*. http://catalogue.ceda.ac.uk/uuid/1f88068e86304b0fbd34456115b6606f

Agencies

- European Space Agency (ESA) Climate Change Initiative (CCI)

Satellite observations

- MODIS Landsurface temperature

Description

The Science use case 2 in Permafrost_cci focuses on the cross-analysis of the existing ESA GlobPermafrost Hot Spot Regions of Permafrost Change (HRPC) product with output from the Permafrost_cci transient permafrost model. The HRPC contains information on Landsat-based trends of landscape disturbances, which may trigger changes in the ground thermal regime or become enhanced by regional to local changes in ground thermal regime.
We hypothesize that climatic fluctuations directly impact permafrost properties and ground thermal regime as measured by active layer thickness (ALT) or permafrost/ground temperature. This in turn will likely impact the initiation and enhancement of permafrost region disturbances (PRD).
Based on this hypothesis we spatially compared the HRPC data products (Nitze et al., 2018 a,b) with the dynamic annual (1997-2018) ALT and PFR (permafrost probability) as well as static permafrost temperature Permafrost CCI+ data products (Obu et al, 2018) for all four core transects of the HRPC data analysis in western Siberia (T1), eastern Siberia (T2), Alaska (T3), and eastern Canada (T4).

Lake drainage - ground temperature relationship

A first cross-analysis between current Permafrost_cci products and GlobPermafrost HRPC disturbance trends focused on the analysis of the spatial relationship between lake drainage and mean annual ground temperature. Lake changes were quantified using trends of multispectral indices of Landsat-time series data from 1999 through 2014 (Nitze et al., 2017, 2018). This includes net lake changes of each individual lake (<1ha) within the transects, as well as the gross increase and decrease (individual fractions of lake area gain and loss). Furthermore, we calculated lake shore change rates in cm per year for each individual lake (n > 600,000).

Lakes in permafrost often exhibit a dynamic behaviour, where lakes often expand over time and ultimately drain once they reach a drainage gradient or permafrost destabilizes. Lake drainage can occur in different magnitudes, where lakes can drain completely or only partially.

Figure 2 shows the relation between net lake area loss of shrinking lakes (negative net lake change) from the HRPC lake change datasets (Nitze et al., 2018b) for all 4 analyzed continental scale permafrost transects. It reveals distinct clusters of lake area loss intensity and mean annual ground-temperature MAGT distributions. All sites show a bimodal distribution of lake area loss, but with different magnitude. The first cluster is typically located at <20 % lake area loss (net change), which is caused by subtle lake fluctuations, data uncertainty, partial lake drainage or a combination of these factors. Lakes with a lake area increase were kept from the analysis. This cluster is the most dominant in T4 (Eastern Canada), which is characterized by mostly stable lake areas across the transect region and thus the permafrost temperature gradient. The second cluster is typically close to 100%, which translates to complete lake drainage. This second cluster is more common in Transects T1-T3, which are more dominated by frozen ice-rich sediments rather than glacially-carved bedrock like T4. The relation of these drainage clusters to MAGT is diverse among the different transects. While T2 is characterized by cold MAGT of predominantly <-4 °C, complete lake drainage events clustered at around -6 °C. In T1 and T3, which have very strong lake dynamics (Nitze et al., 2018a), the complete drainage cluster is close to 0 °C, which may indicate the influence of landscape-scale permafrost degradation and widespread surface permafrost loss in the affected regions. However, regional conditions and differences should be considered and more detailed local to regional-scale analysis will reveal further links between ground temperature, other environmental factors, and the dynamics of permafrost region disturbances such as lake drainages.

Drivers of lake drainage

Furthermore we quantified the impact of environmental variables, such as permafrost, climate, lake shape and geomorphology on lake drainage. We used the RandomForest Feature Importances and SHAP/shapley explainable AI methods (SHAP) based on Random Forest and XGBoost machine learning models. This allowed us to retrogressively model lake drainage and to determine the key drivers of lake drainge and stability for each of the ~600k individual lakes in the HRPC lake dataset.
In this usecase the HRPC dataset served as the main datasource. The CCI Permafrost Ground Temperature dataset v3 (Obu et al., 2019) served as one of the main auxiliary datasets among Climate (ERA5-Land, Copernicus Climate Change Service, 2019), thermokarst characteristics (Olefeldt et al., 2015), IPA permafrost properties (Brown et al., 1997) or geomorphology based on the MERIT DEM (Yamazaki et al., 2017)

Lake shape and local geomorphology are the most important predictors for lake drainage. These correlate very well with lake formation mechanisms and landscape location. Arctic lowland thermokarst lakes e.g., are much more affected by lake drainage than glacially formed lakes on the Canadian shield.

Permafrost and climate variables show a weaker impact on lake drainage. However, ground temperatures between -8 and -3°C show a stronger positive influence on lake drainage, implying a critical threshold of permafrost degradation in this temperature range. Generally, lakes in permafrost are more likely to drain that in thawed soils (>0°C).

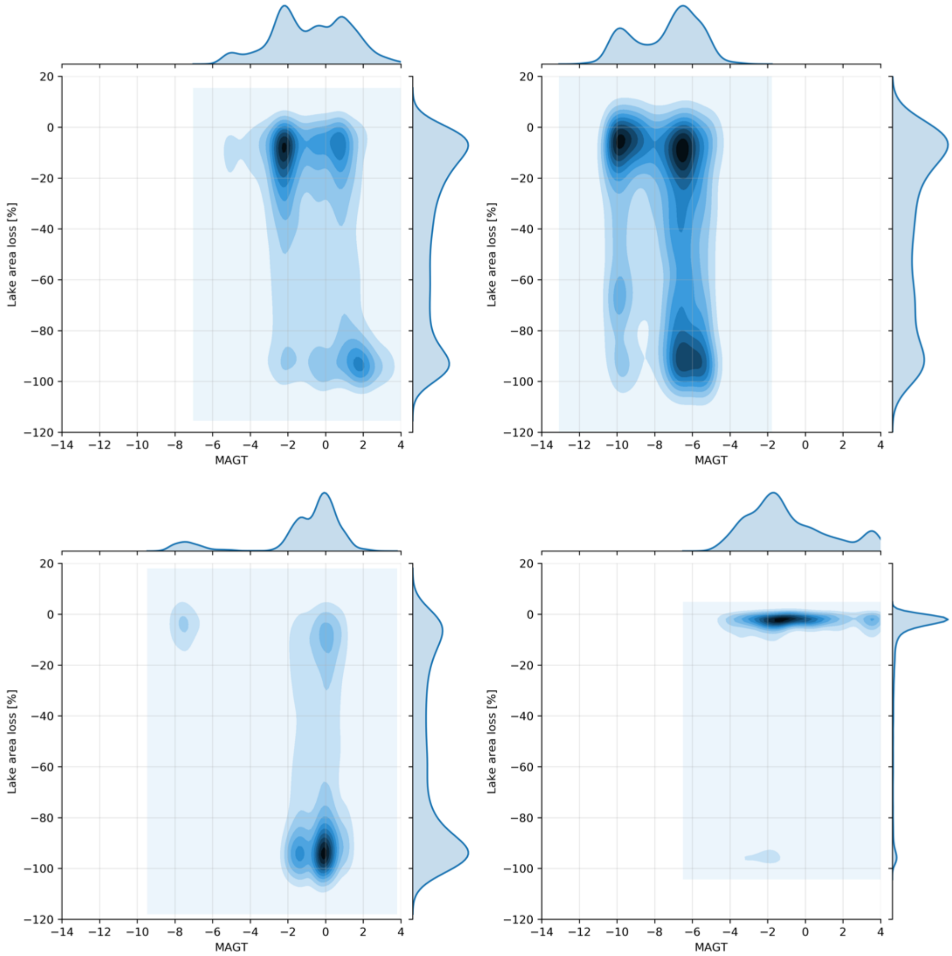

Figure 3: 2D density plots of lake area loss % (per lake) vs. MAGT. Darker colors represent a higher density and thus more lake drainage events. Upper left: T1 Western Siberia; upper right: T2 Eastern Siberia; lower left: T3 Alaska; lower right: T4 Eastern Canada.

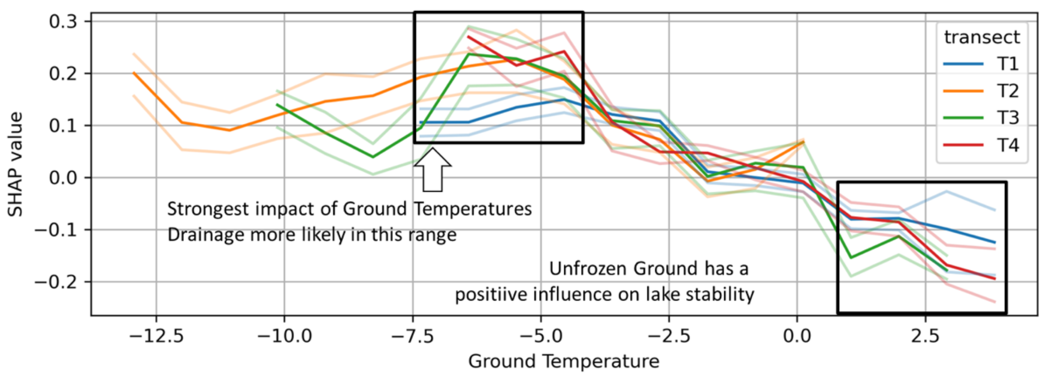

Figure 4. SHAP values (median+-25th and 75th percentile) of ground temperatures for complete drainage (>75% lake area loss). Ground temperatures contribute strongest to lake drainage from -8 to -3 °C. Positive SHAP values (y-axis) indicate a positive influence on lake drainage and vice versa.

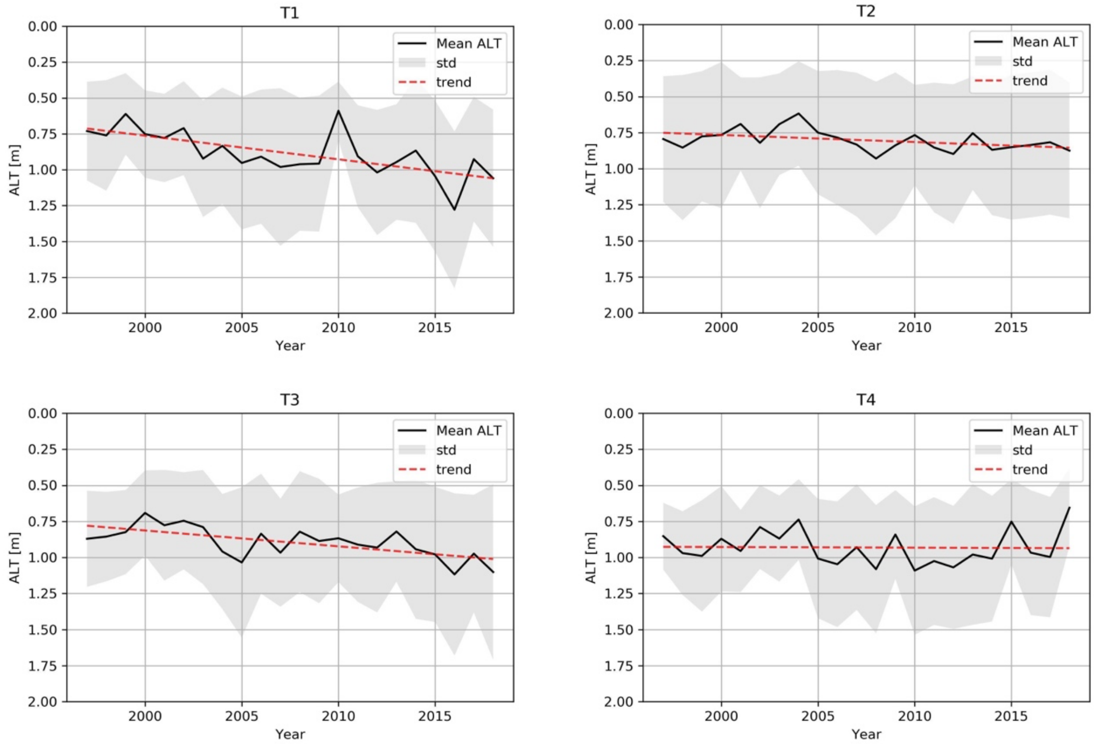

Figure 5. Comparison of Active Layer Thickness dynamics (in meter) in different HRPC Transects (T1: Western Siberia, T2: Eastern Siberia, T3: Alaska, T4: Eastern Canada) derived from annual ALT datasets (1997-2018).

<u>Active layer thickness dynamics</u>

The active layer trends show clear differences between the different transect regions (Figure 5). Transects T1 and T3 show the largest increase in mean ALT, which correlates with the observed lake drainage dynamics. Larger regions within both transects were particularly affected by lake drainage within the past two decades (Nitze et al., 2017, 2018, 2020). Transect T2 was much less affected by ALT deepening, while Transect T4 has a flat trend, although with strong annual fluctuation.

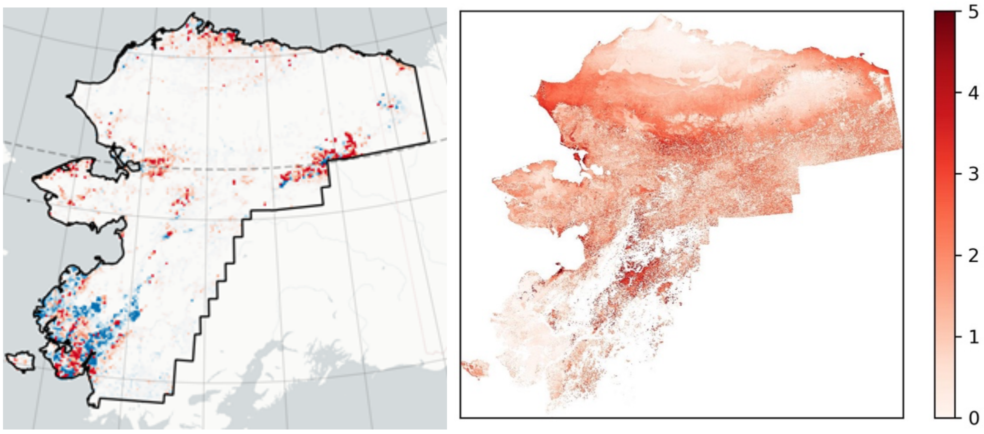

Figure 6: Spatial comparison of (left) Lake area change (1999-2014) from HRPC Datasets and (right) increase in Active Layer Thickness (ALT) trends in % from annual CCI ALT dataset in T3 Alaska.

Wildfire - ALT interactions

Wildfires are a widespread disturbance in the boreal, mostly semi-arid continental permafrost regions such as Central Yakutia, interior Alaska or NW Canada. Two of these regions are located within the HRPC transects T2 and T3. We analyzed the ALT trajectories from 1999 until 2018 within burned areas, non-burned areas and individual fire scars. For this purpose we calculated the mean and standard deviations of annual ALT within the burn scars. Furthermore we applied a linear model to compare the change (slope) in mean ALT and its standard deviation for each region and burn status.

Table 1: Change in mean and standard deviation of Active Layer Thickness in burned and non-burned areas across all 4 transects.

	Fire		No Fire	
Region	*Mean*	*Std*	*Mean*	*Std*
T1	+40.10	+102.23	+49.11	+47.44
T2	+15.45	+21.66	+13.59	+10.11
T3	+30.05	+95.73	+29.74	+59.37
T4	+30.95	+56.63	+0.86	+34.33

Individual Fires

On an individual burn scar level we can directly identify the impact of wildfires. Figure 7 shows the mean (line) and standard deviation (shading) of ALT for the Anaktuvuk River fire scar area from 1999 through 2018. The Anaktuvuk tundra fire in northern Alaska (Jones et al, 2009) burned around 1000 km² (100,000 ha) tundra, partially underlain by ice-rich permafrost, in late summer 2007. Before the large fire in 2007, the mean ALT fluctuated rather strongly (mean ALT 0.53-0.75), depending on annual weather conditions. However, The variance within the analysed site was very low which indicates a rather homogeneous ALT. After the intense tundra fire mean ALT increased to deeper depths (0.7-0.8 m). At the same time the variance of ALT increased markedly within the burned region.

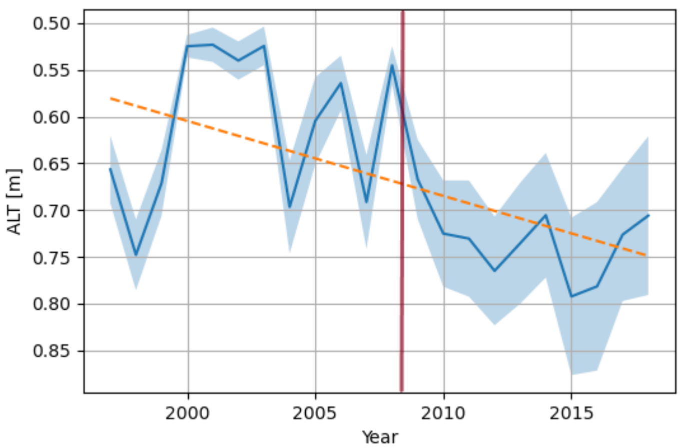

Figure 7: Mean (line), standard deviation (shading) and trend of mean (orange dashed line) of modelled active layer thickness (ALT) within the Anaktuvuk firescar in northern Alaska. Burn date (2007) indicated with a red line.

In all sites, ALT was larger for burned sites than for non-burned sites, which can be expected as wildfires predominantly occur in warmer, forested boreal sites. However, the trajectories of ALT exhibit a different behaviour. In all transects T1-T4, mean ALT increased within burned areas (+15-40%), but also in non-burned areas (+14-49%), except T4 (+1%), with similar magnitudes between burned and non-burned areas (Table 3) . In comparison, variance of ALT increased in burned sites within all transects increased much stronger than in non-burned areas, even (almost) doubling in standard deviation.

Although the impact of wildfire on ALT seems to be much stronger in T4, the impact on ground stability may be much weaker than in the other regions, due to primarily underlying bedrock. We hypothesize a much stronger effect of increasing ALT in e.g. ice-rich permafrost in Alaska (T3) or eastern Siberia (T2). Particularly increasing variance within burned areas, with locally strong increase in ALT, may result in triggering further permafrost disturbances. However, more detailed analysis will be conducted to verify/falsify this hypothesis.

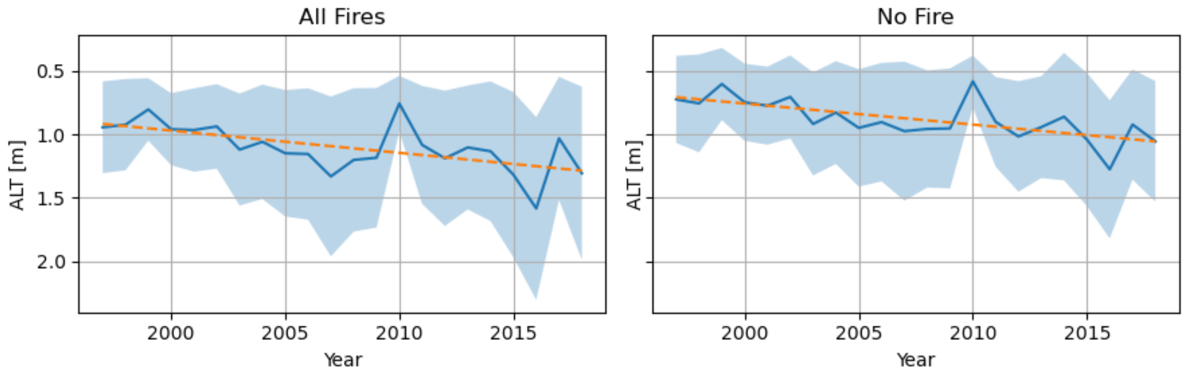

Figure 8: Mean (line), standard deviation (shading) and trend of mean (orange dashed line) of modelled active layer thickness (ALT) in burned and unburned regions in Transect T1 Western Siberia.

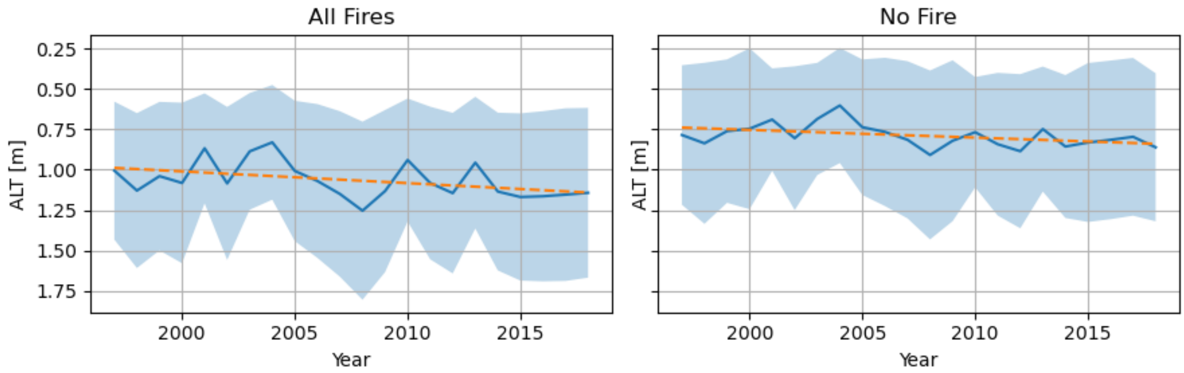

Figure 9: Mean (line), standard deviation (shading) and trend of mean (orange dashed line) of modelled active layer thickness (ALT) in burned and unburned regions in Transect T2 Eastern Siberia.

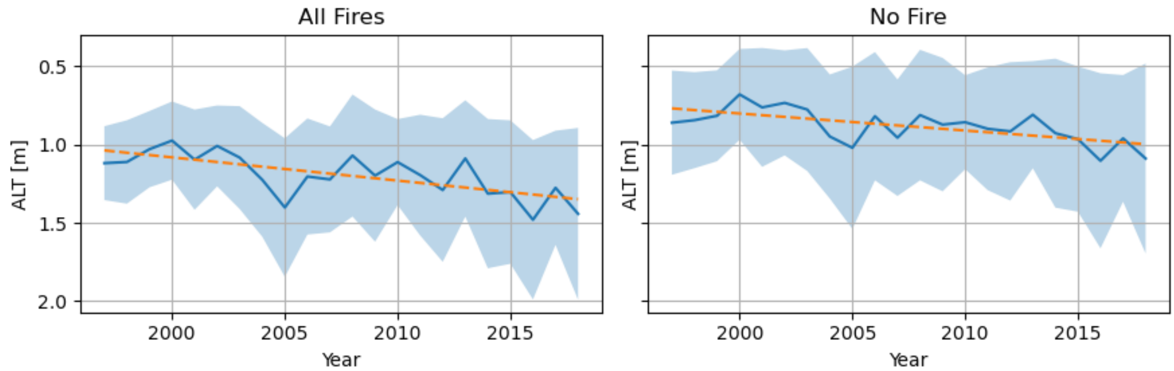

Figure 10: Mean (line), standard deviation (shading) and trend of mean (orange dashed line) of modelled active layer thickness (ALT) in burned and unburned regions in Transect T3 Alaska.

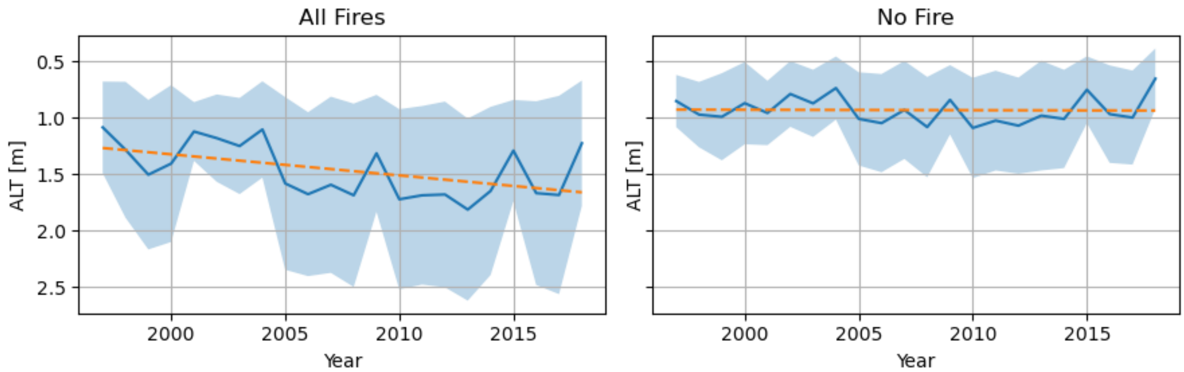

Figure 11: Mean (line), standard deviation (shading) and trend of mean (orange dashed line) of modelled active layer thickness (ALT) in burned and unburned regions in Transect T4 Eastern Canada.

3.4 Use Case Study 3 - Permafrost trends: affected Arctic Infrastructure

- Bartsch, A., Pointner, G., Nitze, I., Efimova, A., Jakober, D., Ley, S., Högström, E., Grosse, G., and Schweitzer, P. (2021): Expanding infrastructure and growing anthropogenic impacts along Arctic coasts, Environmental Research Letters, Volume 16, Number 11, https://doi.org/10.1088/1748-9326/ac3176.

Key points:

- A first panarctic satellite-based record of expanding infrastructure and anthropogenic impacts along all permafrost affected coasts was developed and combined with Permafrost_cci records.
- Almost 97% of all mapped areas showed a positive trend in ground temperature and 93% for ALT.
- 55% of the identified human impacted area will be shifting to above 0 ◦C ground temperature at two meter depth by 2050 if current permafrost warming trends continue at the pace of the last two decades.

Service:

- Adaptation

- Disaster Risk reduction

End user (s)

- Local communities
- Policy makers
- Government agencies
- Researchers

Intermediate user (s)

- Research institutes and academia

Applications

Permafrost is permanently frozen ground. Warming of the Arctic results in widespread increase of ground temperatures and permafrost degradation is occurring in many regions. Trends of Permafrost properties have been combined with a novel Arctic infrastructure database. Settlements prone to change during the last 20 years have been identified and trends have been extrapolated to identify infrastructure which will be affected by diminishing permafrost and potential ground instability by 2050 and 2060 respectively.

Essential Climate Variables

- Cryosphere
    - Permafrost ground temperature
    - Active Layer Thickness

Climate Data Records:
ESA Permafrost Climate Change Initiative (Permafrost_cci): Permafrost version 2 data products, Obu, J.; Westermann, S.; Barboux, C.; Bartsch, A.; Delaloye, R.; Grosse, G.; Heim, B.; Hugelius, G.; Irrgang, A.; Kääb, A.M.; Kroisleitner, C.; Matthes, H.; Nitze, I.; Pellet, C.; Seifert, F.M.; Strozzi, T.; Wegmüller, U.; Wieczorek, M.; Wiesmann, A. (2020): ESA Permafrost Climate Change Initiative (Permafrost_cci): Permafrost version 2 data products. Centre for Environmental Data Analysis, *15.05.2024*. http://catalogue.ceda.ac.uk/uuid/1f88068e86304b0fbd34456115b6606f

Agencies

- European Space Agency (ESA) Climate Change Initiative (CCI)

Satellite observations

- MODIS Landsurface temperature

Description

The accelerating climatic changes and new infrastructure development across the Arctic require more robust risk and environmental assessment, but thus far there was no consistent record of human impact. A first panarctic satellite-based record of expanding infrastructure and anthropogenic impacts along all permafrost affected coasts (100 km buffer, ≈6.2 Mio km2), named the Sentinel-1/2 derived Arctic Coastal Human Impact (SACHI) dataset, was developed and combined with Permafrost_cci records.

An existing processing chain (Bartsch et al 2020a) was used as a first step to obtain results from two different classification approaches. It includes a pixel-based classification using a Gradient Boosting Machine and a windowed semantic segmentation approach (U-Net convolutional neural network architecture) using the deep learning framework Keras with the Tensorflow backend. A Theil-Sen regression was used for trend retrievals from 2 m ground temperature, active layer thickness (ALT), and permafrost fraction. In case of Landsat derived NDVI, the trends have been obtained with Ordinary Least Square regression. For NDVI, changes per decade, and for all other parameters, changes per year were extracted. For each object the average change was derived. This was carried out for all classes together as well as separately. The analyses were made on different levels: the entire Arctic and by country/region (in both cases subset with the 100 km buffer).

At least 15% (180 km2) of SACHI objects correspond to new or increased detectable human impact since 2000 according to a Landsat-based normalized difference vegetation index trend comparison within the analysis extent.

More than 50% of settlements occurs over continuous permafrost and more than 30% over discontinuous permafrost. Most identified areas in Canada and US are located on continuous permafrost. For Russia this applies to less than half of them. Almost 97% of all mapped areas showed a positive trend in ground temperature and 93% for ALT. Temperatures were increasing by 0.8 ◦C per decade on average over the human-impacted area identified within the analysis extent. The ALT increase was 11 cm per decade (average ALT in 2019 was 84 cm). About 8% changed from a permafrost fraction of 100% to a lower value between 1997 and 2019.

The changes in ground temperature during the last two decades tend to be larger in colder permafrost than for ground with temperatures near zero degree C (as determined for the year 2019, figure 12), which agrees with prior findings (Romanovsky et al 2017, Biskaborn et al 2019, Box et al 2019). As the magnitude for the latter is still on the order of one degree C for this time period, the expected impact during the upcoming decades is large if the trend continues. 55% and 67% of human-impacted areas will be located on ground with larger than zero degree C mean annual ground temperature down to 2 m depth in 2050 and 2060 respectively. Most affected is Russia and some areas in the US (Alaska) (figure 13).

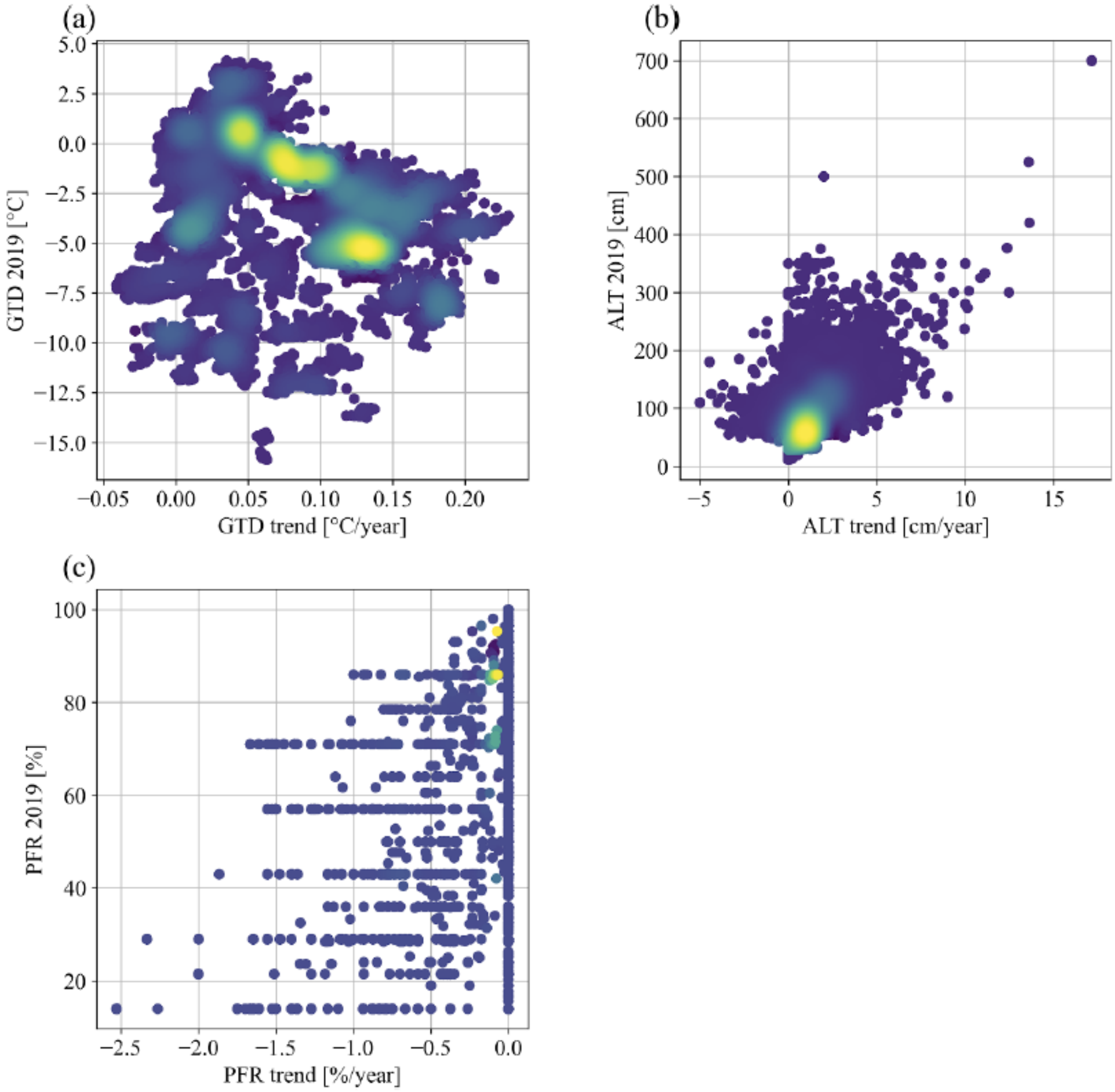

Figure 12: Scatterplots of trend versus 2019 status for (a) ground temperature at 2 m depth, (b) active layer thickness and (c) permafrost fraction. Each point represents the average for a distinct object (human impacted area) as mapped with Sentinel-1 and -2 (Bartsch et al 2021b, dataset on ZENODO). Calculations are based on Obu et al (2021a, 2021b, 2021c) respectively. (Source: Bartsch et al. 2021a, ERL)

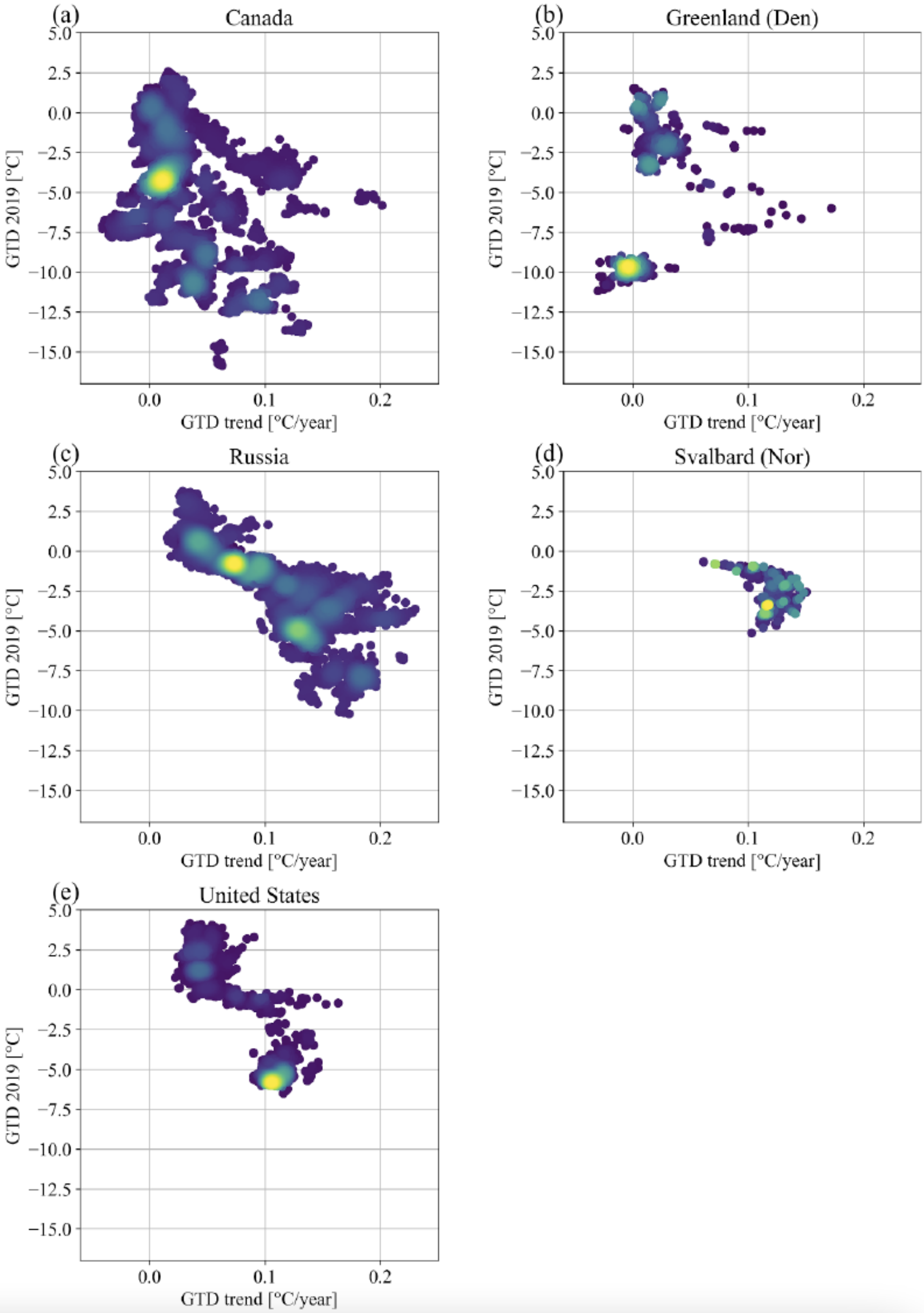

Figure 13: Scatterplots of ground temperature (GTD; 2 m depth) trend versus 2019 status for different countries/regions (analysis extent only). Each point represents the average for a distinct object (human impacted area) as mapped with Sentinel-1 and -2 (Bartsch et al 2021b). (Source: Bartsch et al. 2021a, ERL)

3.5 Use Case Study 4 – Analysis of Permafrost_cci Rock Glacier Inventories (RoGI)

Bertone, A., Barboux, C., Bodin, X., Bolch, T., Brardinoni, F., Caduff, R., Christiansen, H. H., Darrow, M. M., Delaloye, R., Etzelmüller, B., Humlum, O., Lambiel, C., Lilleøren, K. S., Mair, V., Pellegrinon, G., Rouyet, L., Ruiz, L., and Strozzi, T.: Incorporating InSAR kinematics into rock glacier inventories: insights from 11 regions worldwide, The Cryosphere, 16, 2769–2792, https://doi.org/10.5194/tc-16-2769-2022, 2022.

Key points:

- Spaceborne InSAR is able to systematically document rock glacier creep rate in regional inventories (RoGI products). The kinematic attribute is useful to refine the activity assessment.
- The international standards for inventorying rock glaciers allow for providing comparable RoGI products in various regions around the globe.
- Remaining discrepancies mostly attributed to operator subjectivity may be mitigated by adjusting the RoGI procedure.

Service:

- Adaptation
- Disaster Risk reduction

End user (s)

- Local communities
- Government Agencies
- Researchers

Intermediate user (s)

- Research institutes and academia

Applications

The Use Case analyses the Rock Glacier Inventory (RoGI) products delivered in the Climate Research Data Package (CRDP) from the European Space Agency Climate Change Initiative (ESA CCI) Permafrost (https://climate.esa.int/en/projects/permafrost/). The study evaluates the value of using spaceborne Interferometric Synthetic Aperture Radar (InSAR) based on Sentinel-1 SAR and ALOS2 PALSAR-2 images, to assign a kinematic attribute to the inventoried landforms and improve the assessment of rock glacier activity.

Essential Climate Variables

- Cryosphere
  - Permafrost – rock glacier kinematics

Climate Data Records

[RD-10] Rouyet, L., Echelard, T., Schmid, L., Pellet, C., Delaloye, R., Onaca, A., Sirbu, F., Poncos, V., Brardinoni, F., Kääb, A., Strozzi, T., Jones, N., Bartsch, A. 2023. ESA CCI+ Permafrost Phase 2 – CCN4 Mountain Permafrost: Rock Glacier Inventories (RoGI) and Rock glacier Velocity (RGV) Products. D3.2 Climate Research data Package (CRDP), v1.0. European Space Agency. https://climate.esa.int/documents/2365/CCI_PERMA_PhaseII_RG_D3.2_CRDP_v1.0.pdf

Agencies

- European Space Agency (ESA) Climate Change Initiative (CCI)
- Department of Biological, Geological and Environmental Sciences, University of Bologna, Bologna, 40126, Italy
- Department of Geosciences, Geography, University of Fribourg, Fribourg, 1700, Switzerland
- Laboratoire EDYTEM, CNRS/Université Savoie Mont-Blanc, Le Bourget-du-Lac, 73370, France
- School of Geography & Sustainable Development, University of St Andrews, St Andrews, KY16 9AL, United Kingdom
- Gamma Remote Sensing, Gümligen, 3073, Switzerland
- Arctic Geology Department, The University Centre in Svalbard, Longyearbyen, P.O. Box 156, 9171, Svalbard, Norway
- Department of Civil, Geological, and Environmental Engineering, University of Alaska Fairbanks, Fairbanks, Alaska 99775-5900, USA
- Department of Geosciences, University of Oslo, Oslo, 0316, Norway
- Institute of Earth Surface Dynamics, University of Lausanne, Lausanne, 1015, Switzerland
- Office for Geology and Building Materials Testing, Autonomous Province of Bolzano, Bolzano, 39100, Italy
- Energy and Technology Department, NORCE Norwegian Research Centre AS, Tromsø, 9294, Norway
- Argentine Institute of Nivology, Glaciology and Environmental Sciences, CCT CONICET Mendoza, Mendoza, 5500, Argentina

Satellite observations

- Sentinel-1
- ALOS-2 PALSAR-2

Description

The use case study #4 focuses on inter-comparing the findings of the Rock Glacier Inventories (RoGIs) generated in Permafrost_cci Phase 1 (CRDP CCN2, [RD-15]) and evaluates the value of using InSAR to assign a kinematic attribute to the inventoried rock glaciers. The findings are presented and discussed in a scientific article published in The Cryosphere (Bertone et al., 2022).

The RoGIs from the 11 regions of Permafrost_cci CCN2 (Option 1 and Option 4) are compared. Three regions are in the European Alps: western Swiss Alps (Switzerland), southern Vinschgau/Venosta Valley (Italy) and Vanoise Massif (France). Five areas are in the sub-Arctic and high-Arctic regions: Troms and Finnmark (northern Norway), Nordenskiöld Land (Svalbard), Disko Island (Greenland) and Brooks Range (Alaska, USA). One region is in Central Asia: northern Tien Shan (Kazakhstan).

It should be noted that the RoGI procedure and RGIK reference guidelines have been in constant evolution and have therefore iteratively been updated and improved based on the identified limitations. The workflow presented by Bertone et al. (2022) (Figure 14) corresponds to the methodology presented in the CCN2 ATBD in 2020 [RD-16], in agreement with the versions of the RGIK guidelines released in 2022.

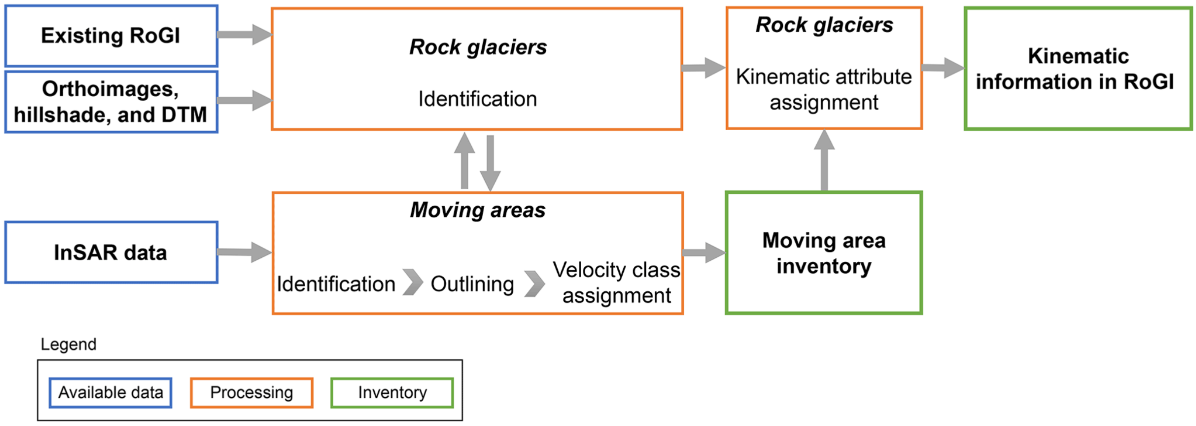

Figure 14: Standardised method presented in Bertone et al., (2022) to produce InSAR Moving Areas (MAs) and RoGIs that include a kinematic attribute (Bertone et al., 2022).

The analysis focused on 5077 InSAR-based Moving Areas (MAs) corresponding to 5140 km^2 within the study areas (total surface: 31500 km^2), and the kinematic attributes assigned to the 3666 identified Rock Glaciers (RoGs) (CRDP CCN2, [RD-15]). The numbers of identified RoGs and related MAs vary between region, depending on their extent and geomorphological characteristics (Figure 15). The morpho-kinematic attributes documenting the characteristics of the inventoried RoGs were systematically compared between the regions (e.g. Figure 16), to discuss the value and drawbacks of the applied methodology and resulting products.

The study identified several limitations. First, there is a level of subjectivity in the way each operator interpreted the guidelines, which led to variable and not necessarily comparable products due to the few operators involved in the RoGI generation during Permafrost_cci Phase 1. This conclusion led to the design of the multi-operator exercise performed in Permafrost_cci Phase 2. Second, relict landforms were treated differently between the study areas. In some regions, a pure kinematic-approach had been applied, focusing only on landforms where an associated MA has been identified. In other regions, initial geomorphological inventories based on optical imagery and/or field observations were used, and all types of activity were therefore included. This discrepancy led a revised version of the RoGI workflow (geomorphological approach used for the identification rock glaciers, performed in parallel to the InSAR-based MA delineation) for the exercise performed during Permafrost_cci Phase 2. Finally, different InSAR input data (single interferograms vs stacking maps) and ways to classify the velocity (manual or semi-automated) were used in each region. This discrepancy has also been mitigated in Phase 2 by requiring a manual MA delineation based on a larger variety of data inputs in all study areas.

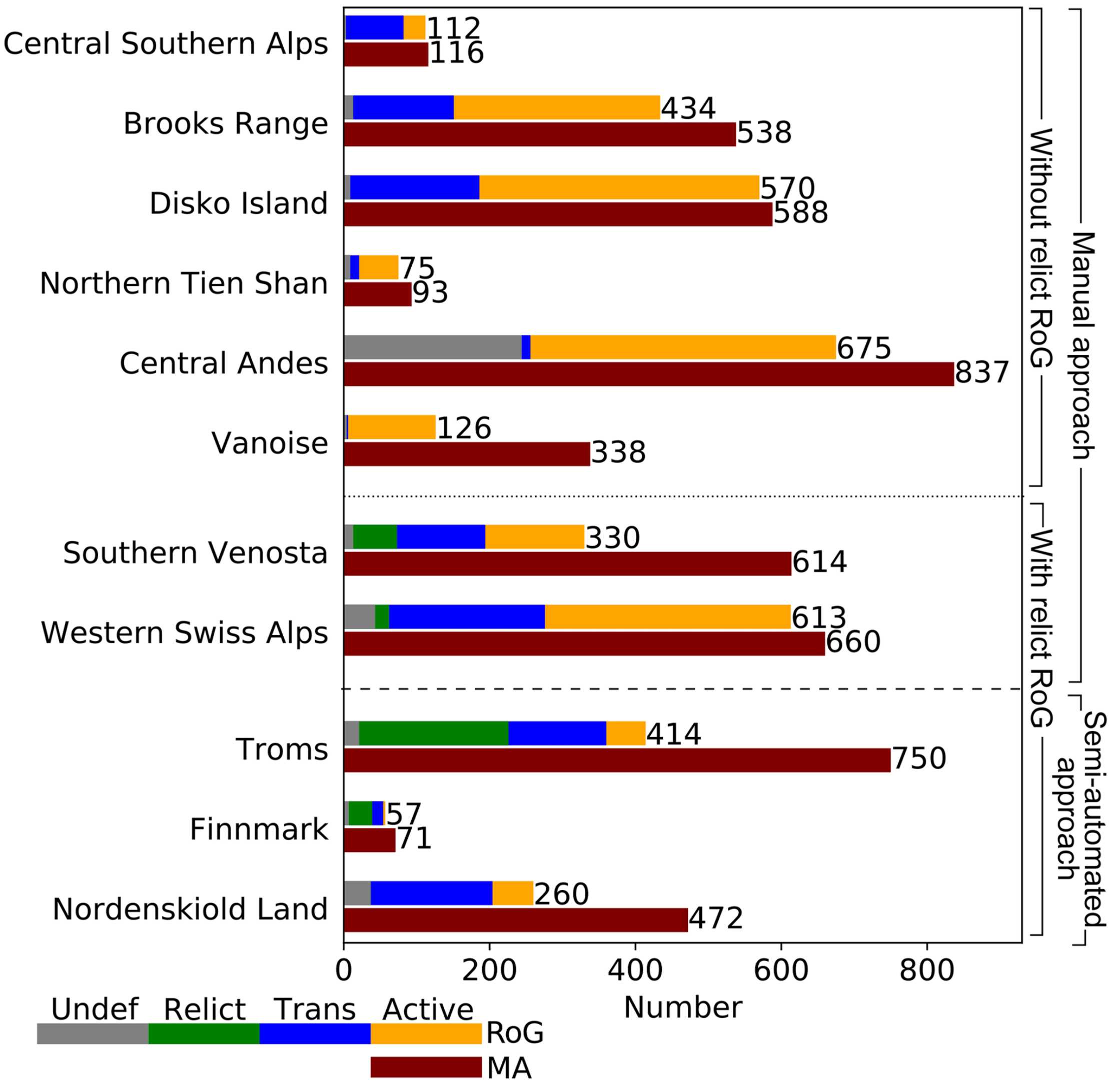

Figure 15: Number of inventoried MAs (dark red bars) and rock glaciers (RoGs) classified as undefined (grey bars), relict (green bars), transitional (blue bars) and active (orange bars) for each investigated region. The length of the bars is proportional to the number of observations. The numbers on the right of each bar indicate the total number of MAs and RoGs. The regional RoGIs are separated according to (i) the method used for mapping the MAs (manual or semi-automated) and (ii) the inclusion or exclusion of relict landforms.

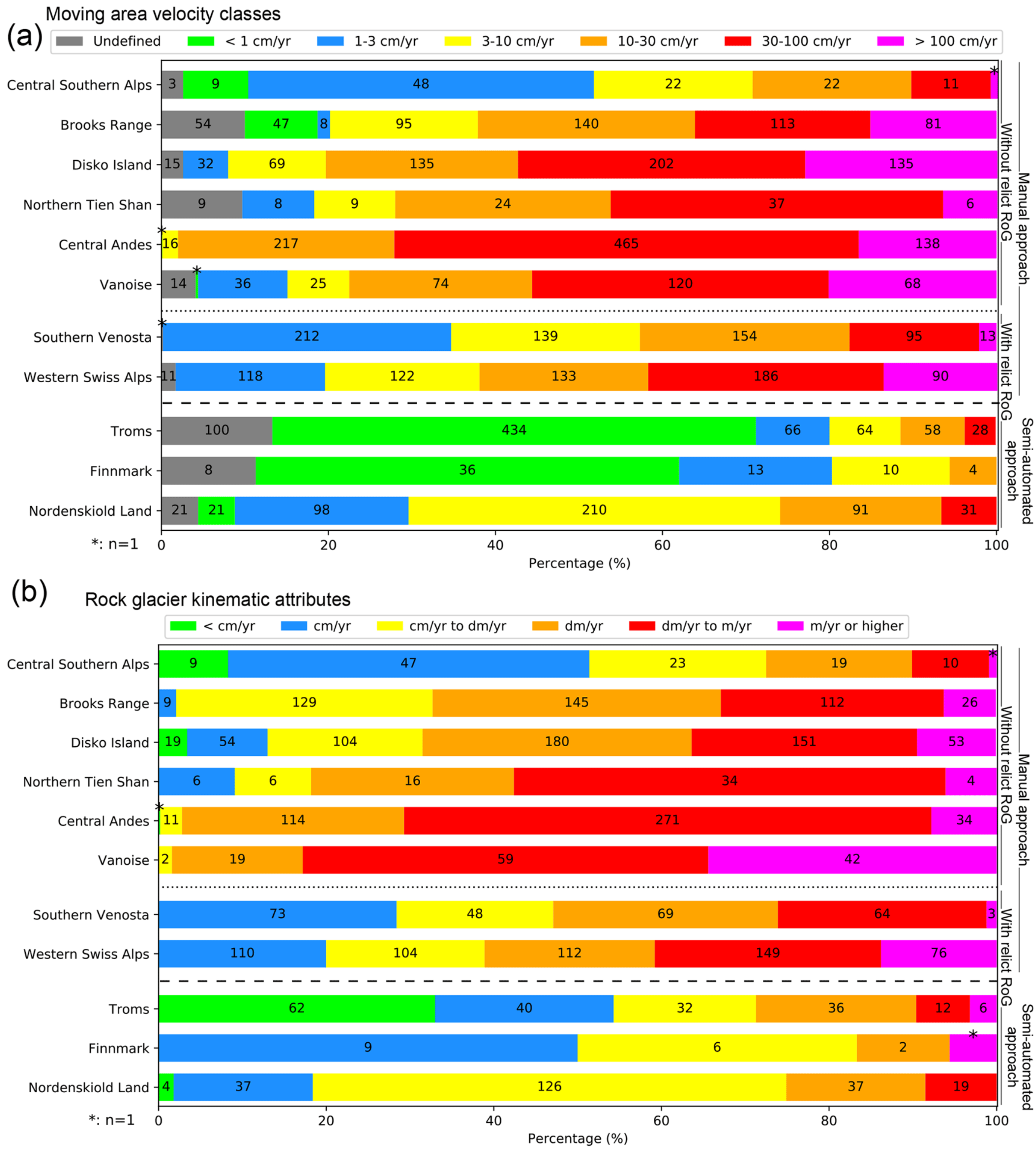

Figure 16: Assigned MA velocity classes (a) and RoG kinematic attributes (b) for each investigated region. The length of the bars is proportional to the percentage, and the values inside the bars indicate the numbers for each category. The regional RoGIs are separated according to (i) the method used for mapping the MAs (manual or semi-automated) and (ii) the inclusion or exclusion of relict RoGs.

.5 Further documented use

Permafrost_cci ground temperature

- Bartsch, A., Strozzi, T., and Nitze, I.: Permafrost Monitoring from Space, Surveys in Geophysics, 2023. https://link.springer.com/article/10.1007/s10712-023-09770-3.

- Miner, K., Turestky, M., Malina, E., Bartsch, A., Tamminen, J., McGuire, A.D., Fix, A., Sweeney, C., Elder, C.D., and Miller, C.E. (2022): Permafrost carbon emissions in a changing Arctic, Nature Reviews Earth & Environment, 3, 55–67. https://doi.org/10.1038/s43017-021-00230-3.
- Bartsch A, Ley S, Nitze I, Pointner G and Vieira G (2020), Feasibility Study for the Application of Synthetic Aperture Radar for Coastal Erosion Rate Quantification Across the Arctic. Front. Environ. Sci. 8:143. doi: 10.3389/fenvs.2020.00143. https://www.frontiersin.org/articles/10.3389/fenvs.2020.00143/full

Permafrost_cci active layer thickness

- Brouillette, M. (2021). How microbes in permafrost could trigger a massive carbon bomb. Genomics studies are helping to reveal how bacteria and archaea influence one of Earth's largest carbon stores as it begins to thaw. News Feature. *Nature*, *591*(7850), 360–362. https://doi.org/10.1038/d41586-021-00659-y
- Tamm., J. (2021): Remote-sensing based assessment of post-fire changes in land surface temperature in Arctic-Boreal permafrost regions. Master Thesis, University of Potsdam. 74pp.

GlobPermafrost Permafrost extent use examples

- Ramage, J., Jungsberg, L., Wang, S., Westermann, S., Lantuit, H. & Heleniak, T. (2021), 'Population living on permafrost in the Arctic', *Population and Environment*. https://doi.org/10.1007/s11111-020-00370-6
- Julian Murton, Periglacial Processes and Deposits, Editor(s): David Alderton, Scott A. Elias, Encyclopedia of Geology (Second Edition), Academic Press, 2021, 857-875, ISBN 9780081029091, https://doi.org/10.1016/B978-0-12-409548-9.11925-6
- Kåresdotter, E., Destouni, G., Ghajarnia, N., Hugelius, G., & Kalantari, Z. (2021). Mapping the vulnerability of Arctic wetlands to global warming. *Earth's Future*, 9, e2020EF001858. https://doi.org/10.1029/2020EF001858
- Lapierre Poulin, F., Fortier, D., & Berteaux, D. (2021). Low vulnerability of Arctic fox dens to climate change-related geohazards on Bylot Island, Nunavut, Canada. *Arctic Science*, 1–16. https://doi.org/10.1139/as-2019-0007
- Webb, E. E., Loranty, M. M., & Lichstein, J. W. (2021). Surface water, vegetation, and fire as drivers of the terrestrial Arctic-boreal albedo feedback. *Environmental Research Letters*, 16(8), 084046. https://doi.org/10.1088/1748-9326/ac14ea
- Horizon2020 project Nunataryuk (GRID Arendal): Foldable map of permafrost around the world https://www.grida.no/news/13
- Ardelean, F., Onaca, A., Chețan, M.-A., Dornik, A., Georgievski, G., Hagemann, S., Timofte, F., & Berzescu, O. (2020). Assessment of Spatio-Temporal Landscape Changes from VHR Images in Three Different Permafrost Areas in the Western Russian Arctic. *Remote Sensing*, 12(23), 3999. https://doi.org/10.3390/rs12233999

Climate modelling:

- Burke, E.J., Zhang, Y., Krinner, G. (2020): Evaluating permafrost physics in the Coupled Model Intercomparison Project 6 (CMIP6) models and their sensitivity to climate change, *The Cryosphere*, 14, 3155–3174, 2020, https://doi.org/10.5194/tc-14-3155-2020

3.6 Permafrost_cci utility based on evaluation results for GRD, ALT and EXT

This science case study is the utility assessment of the Permafrost_cci ECV products. The independent validation is carried out with strong support of the user community, with in situ measurements characterised by community-wide management best practices with open data access and a collaborative user environment within an international framework: WMO and GCOS delegated the global monitoring of the ECV Permafrost to the Global Terrestrial Network for Permafrost (GTN-P) that is managed by the International Permafrost Association (IPA). GTN-P/IPA established the Thermal State of Permafrost Monitoring (TSP) for permafrost temperature and the Circumpolar Active Layer Monitoring program (CALM) for active layer thickness monitoring. The national-wide Russian meteorological monitoring network ROSHYDROMET additionally provides long-term ground temperature records close to meteorological stations. GTN-P and ROSHYDROMET time series and data collections from additional networks provide reference data sets, however no easy-to use or readily available time-series depth data that are data-fit for validation. We assembled standardised reference data from 1997 to 2021 spanning permafrost regions from Scandinavia to higher latitude permafrost and all altitude ranges from lowland to mountain permafrost across a wide range of latitudes, altitudes, climate zones, land cover, and lithologies.

Permafrost_cci CRDPv3 provides 1 km pixel resolution ECV products on mean annual ground temperature (MAGT) at discrete depths (product name GTD), Active Layer Thickness (product name ALT) and Permafrost Fraction (product name PFR). All products cover the Northern hemisphere north of 30 °N. Permafrost_cci GTD, ALT and PFR time series from 1997 to 2021 come with an annual resolution. The growing demand for mapped permafrost products needs to accommodate user requirements that span permafrost regions from Scandinavia, Mongolia, China to higher latitude permafrost in North America, Greenland, Siberia and all altitude ranges from lowland to mountain permafrost. This results in high difficulties of assessing how the Permafrost_cci products perform in all regions across a wide range of latitudes, altitudes, climate zones, land cover, and lithologies.

Permafrost_cci products are evaluated using standard match-up statistical approaches, supported by expert knowledge. The match-ups were executed using a pixel-based approach. Permafrost_cci GTD is provided in 0.0, 1.0, 2.0, 5.0, and 10.0 m depth and depth-interpolated to fit the depths of the extensive in situ data set. The match-up data is highly standardized, but still contains a large variability of match-up pairs in time, region, and MAGT reference depths. The mountain permafrost monitoring program PERMOS in Switzerland is specifically assessing the Permafrost_cci products for high-mountain permafrost regions, using in situ observations of surface temperature and borehole temperatures and the ESA GlobPermafrost slope movement inventory in the Swiss Alps and the Permafrost_cci rock glacier inventory in the Alps and worldwide at case study sites. In addition, the validation and evaluation efforts innovatively apply the Freeze-Thaw to Temperature (FT2T) product, an EO microwave-derived ground temperature, for comparison with the Permafrost_cci permafrost temperature product.

Permafrost_cci GTD match-up evaluation between simulated Permafrost_cci and in situ measurements showed the following performance characteristics: Permafrost_cci GTD match-up evaluation shows a median bias of -0.89 °C (mean bias -0.73 °C) for the circum-arctic. Geographically, a relatively large proportion of residuals >95% & <5% quantile of the bulk data set is located in the mountainous regions of southern Alaska and western Canada, while a large share of <5% residuals is found in northern Alaska and eastern Russia. The Permafrost_cci GTD < 1 °C group shows a much better performance than the bulk dataset, with a median bias of 0.38 °C (mean bias 0.15 °C) for all depths, and a median bias of 0.32 °C (mean bias 0.08 °C) for all depths excluding the surface temperature at 0 m depth.

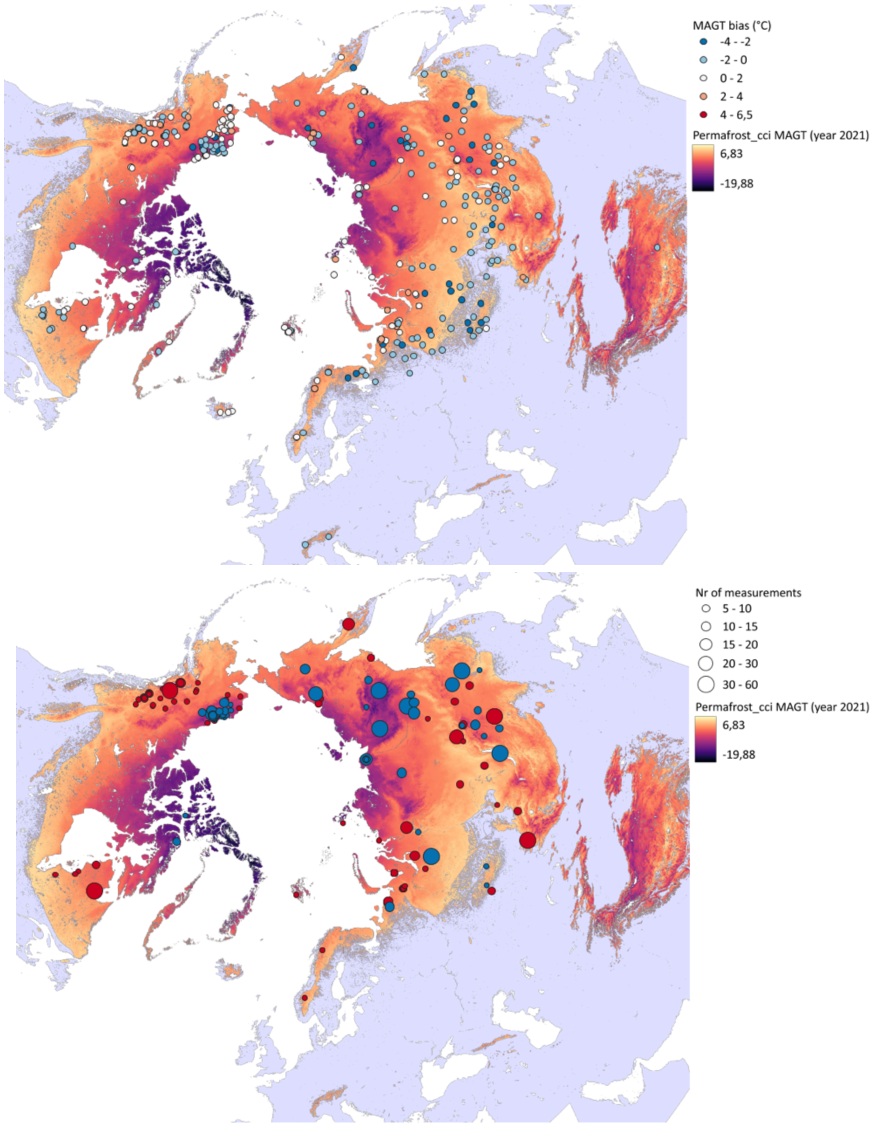

Figure 17: Bias (upper panel) and location of residuals > 95% quantile (red) and < 5% quantile (blue) over mapped Permafrost_cci MAGT (2 m). The size of the circle represents the number of samples with specific residuals at the particular location.

Overall, the majority of match-up pairs (83.89 % for case PFR<=14 and 87.99 % for case PFR <=29 %) are in agreement between the in-situ proxy for permafrost abundance yes / no and Permafrost_cci abundance yes / no. Notably, the 100 % and the 0 % PFR show high percentage of agreement, with 98.61 % and 97.88 % match, respectively. Geographically, most mismatches are located in the Eurasian and Canadian southern boundary of the permafrost extent. The high agreement in the 100 % and 0 % Permafrost_cci PFR groups is stable across years.

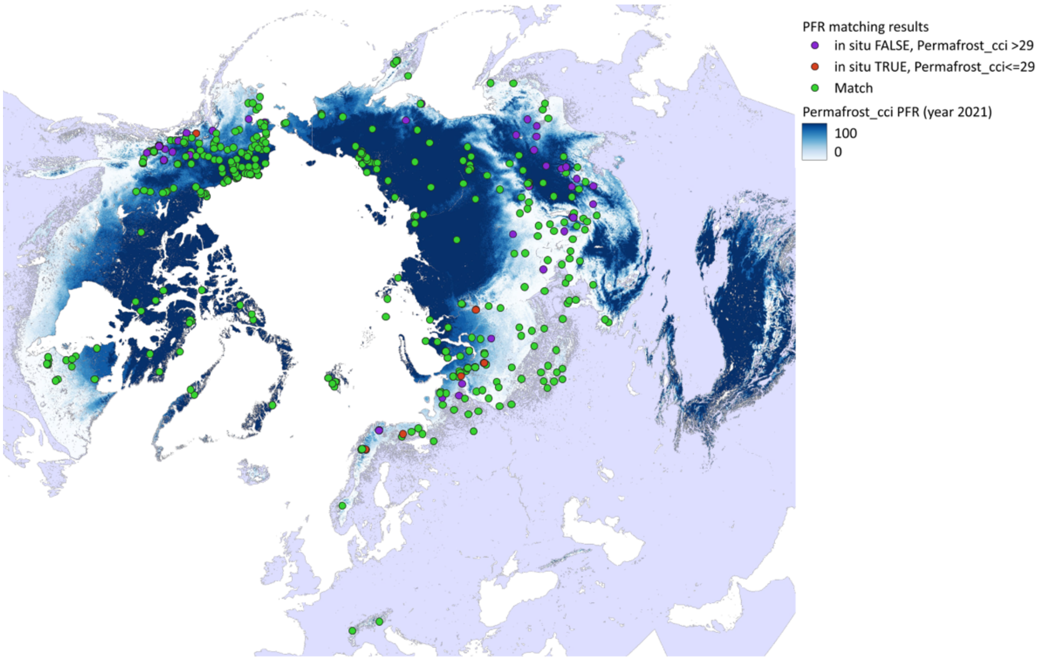

Figure 18: Spatial distribution of PFR match-up pairs grouped by matching characteristics over mapped Permafrost_cci PFR.

For the Permafrost_cci ALT match-up analyses, we restricted the analysis on high-latitude to mid-latitude permafrost regions related to the Permafrost_cci model parameterization, excluding all sites in Mongolia, Central Asia, on the Tibetan Plateau (China) due to their different snow and subground regimes. Permafrost_cci ALT performance with match-up pairs from China and Mongolia excluded is characterised by a median bias of -13cm (95% CI: -90 to 48 cm). A larger bias > 1 m (deep Permafrost_cci ALT versus shallow in situ ALT) occurs only in a few match-up pairs in Alaska, Canada and Russia and Permafrost_cci bias <-1.5 m mainly occurs in Svalbard (shallow Permafrost_cci ALT versus deep in-situ ALT). The mean temporal stability (ts, year-year change in magnitude of the bias*)* show stable ranges around -0.2 cm, with variation mainly in the range of +/- 50 cm and gleichläufigkeit (glk, fraction of same-directional year-to-year changes) shows a robust temporal stability around 60 %.

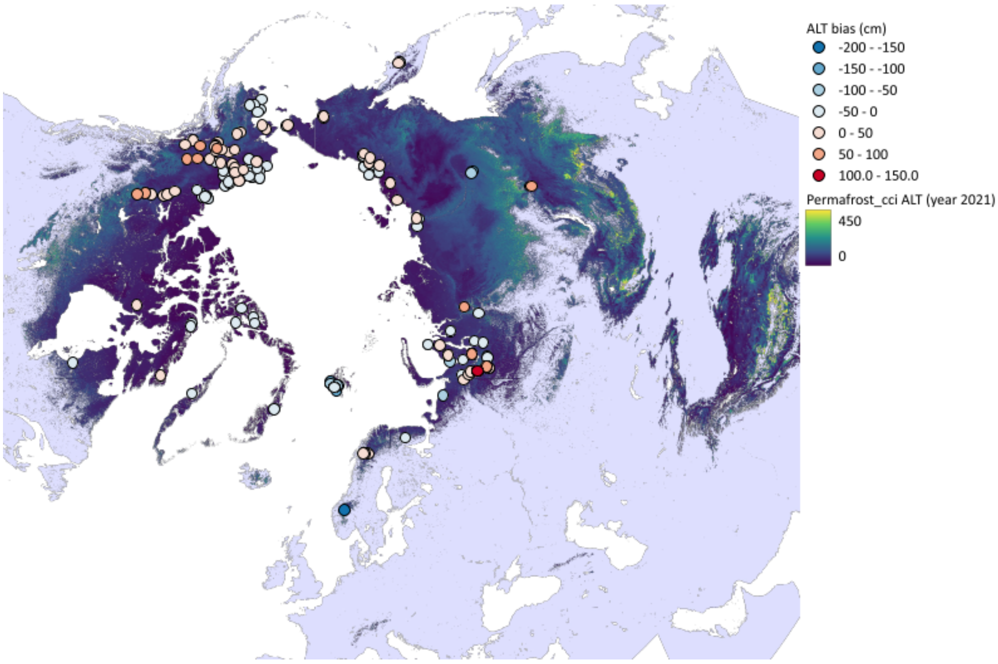

Figure 19. Spatial distribution of mean bias per site from Permafrost_cci ALT and in situ ALT match-up over mapped Permafrost_cci ALT in cm.

PERMOS investigations in the Swiss Alps showed that the performance of Permafrost_cci GTD and Permafrost_cci PFR highly improved for mountain regions. Permafrost_cci GTD shows a slight cold bias of -0.265°C only. At larger depth, Permafrost_cci GTD shows a slight warm bias of +0.275°C at 10 m depth. Permafrost_cci GTD fits best with the in situ observations near the surface with the bias increasing with depth at all sites. Although the absolute values are different, both the in situ measurements and Permafrost_cci GTD show the consistent warming trend over the period 1997-2021. Permafrost_cci GTD matches some of the inter-annual variability (i.e. warmer GTD due to the extreme warm years in 2003 and 2015) but not the cooling events due to snow effects. At depth, measured in situ MAGT in 2017 shows a more or less marked cooling effect due to the extremely snow-poor winter 2016/17 in the Swiss Alps, which enabled the cold winter air temperature to cool the ground more efficiently. This effect is not matched in Permafrost_cci GTD, illustrating the difficulty to include the winter snow effects in mountain regions.

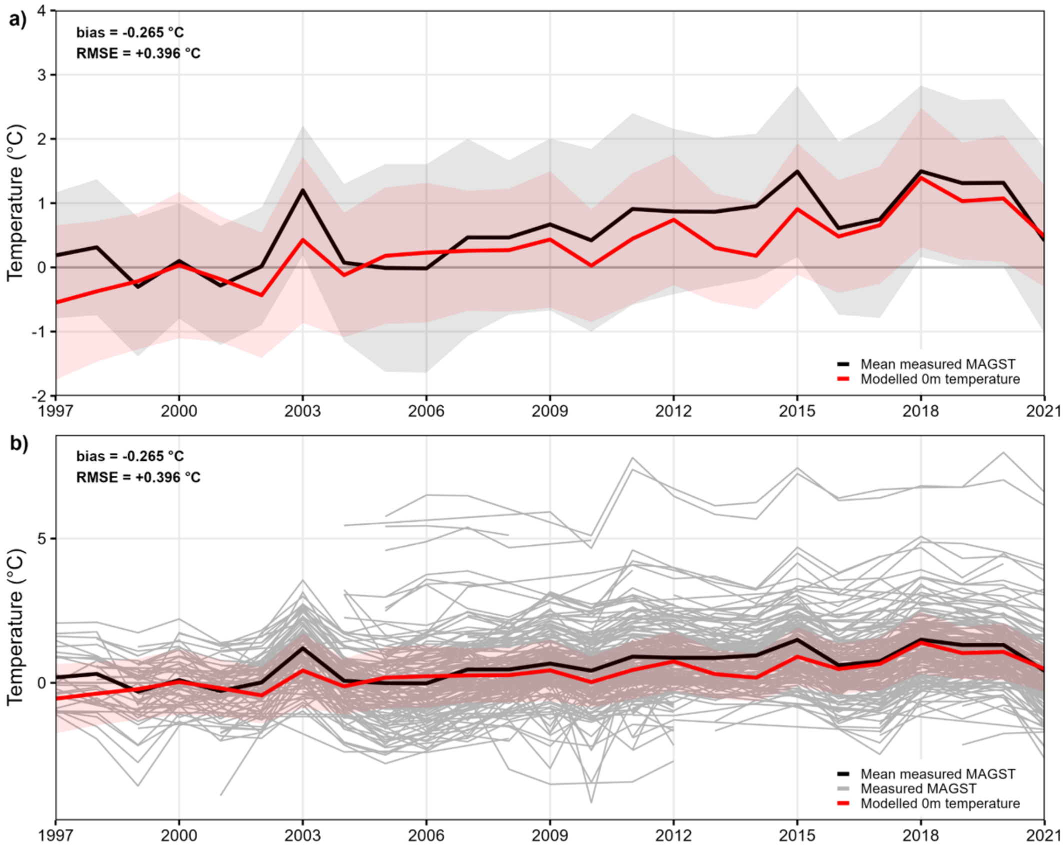

Figure 20. Temporal evolution of the mean in situ measured MAGST (black) in Switzerland (a) and measured MAGST at each logger (b) compared to the mean Permafrost_cci GTD at 0 m depth (red) over the entire Swiss Alps between 2500 and 3000 m a.s.l. The shaded area represents ± one standard deviation.

However, due to the major improvement in Permafrost_cci GTD, also the Permafrost_cci PFR product matches now the large majority of inventoried ESA GlobPermafrost slope movement products are located within Permafrost_cci PFR permafrost extent, as well as 11 amongst the 12 PERMOS permafrost borehole sites in the Alps are located within Permafrost_cci PFR permafrost extent. The majority of inventoried ESA GlobPermafrost slope movement products and Permafrost_cci rock glacier products that were located outside of the Permafrost_cci PFR in phase I before. Permafrost_cci PFR also performs well in the 10 regions where Permafrost_cci rock glacier inventory products are available for the Northern hemisphere.

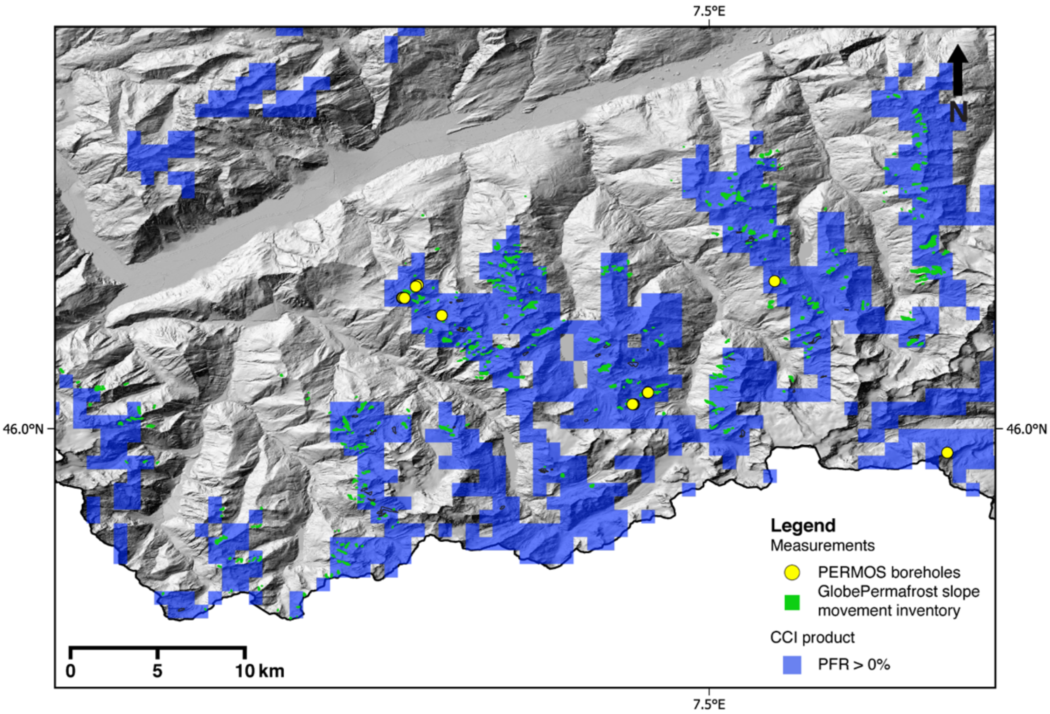

Figure 21. Overview of the simulated Permafrost_cci PFR in 2021 in Bas-Valais (CH) compared to the ESA GlobPermafrost slope movement inventory and PERMOS permafrost monitoring borehole locations.

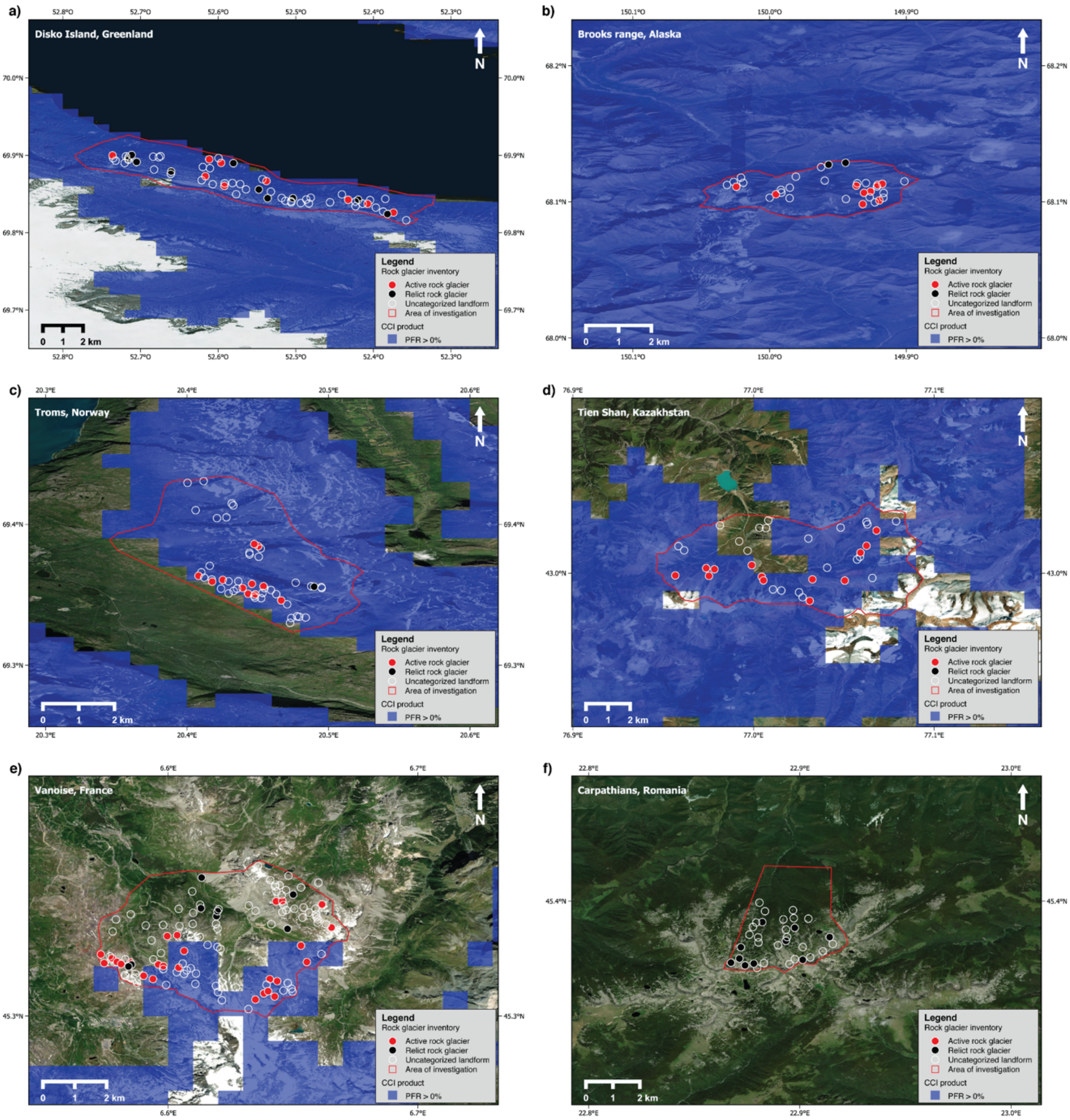

Figure 22: Overview of the simulated Permafrost_cci PFR in 2021 compared to the Permafrost CCI Phase 1 rock glacier inventories in Disko Island (a), Brooks range (b), Troms (c), Tien Shan (d), Vanoise (e) and Carpathians. The active rock glaciers (i.e. currently affected by permafrost creep) are indicated in red and the relict rock glaciers (i.e. formerly affected by permafrost creep) are in black. Uncertain and uncategorized landforms are indicated with hollow circles

Ground temperatures based on satellite-derived freeze/thaw (FT2T) agree at selected cold sites for the overlap period 2008-2018 for CRDPv1. Deviations occur in the permafrost transition zone. In the presented cases, only one product (either CRDPv1 or FT2T) agrees with in situ measurements. A bias of about 1.5°C can be observed for Alaska as well as Greenland for CRDPv2.

In summary, the Permafrost_cci permafrost temperature (that we define as GTD < 1°C) shows good performance with a median bias of 0.35 °C for all depth layers and is well usable by the climate research community. Users of Permafrost_cci GTD products should consider that Permafrost_cci GTD > 1 °C outside of the permafrost zones is characterised by a cold median MAGT bias of -1.17 °C (mean bias -1.11 °C). This leads in turn to and an overestimation of the areal extent of permafrost (especially in the Permafrost_cci PFR= 29 % class) at the southern boundaries of Permafrost in discontinuous, and sporadic permafrost regions.

We consider Permafrost_cci GTD and PFR products for the Northern hemisphere to be most reliable in the permafrost temperature range with GTD < 1 °C and in PFR > 50% as well as PFR <= 29% is reliable as non-permafrost.

3.7 Assessment of utility of Rock Glacier Inventory (RoGI) Products

The RoGI multi-operator exercise performed between June and November 2023 resulted in a dataset of InSAR-based Moving Areas (MA), Rock Glacier Unit (RGU) Primary Markers (PM) and outlines for all the 12 selected areas [RD-12]. The assessment is based on feedbacks from the PIs from 10 institutions in 8 countries: The University of Fribourg (Switzerland), Gamma Remote Sensing AS (Switzerland), NORCE Norwegian Research Centre (Norway), The University of Bologna (Italy), West University of Timisoara (WUT) (Romania), The University of Savoie Mont-Bland / The University of Grenoble Alps (France), The University of Alaska Fairbanks (USA), Argentine Institute of Nivology, Glaciology and Environmental Sciences (IANGLA) (Argentina), Graz University of Technology (TU Graz (Austria) and The University of Lausanne (Switzerland). The comments of the results and RoGI process are based on several rounds of discussions with a large group of operators (5–10 operators in each area, 40 persons in total). The primary conclusions, strengths and limitations of the produced RoGI are detailed in the PVIR [RD-13] and PUG [RD-14].

The feedbacks from the PIs and operator teams are overall very positive. The steps and instructions of the exercise were generally assessed as clear and easy to follow. Most PIs/teams reported that they liked the structure and clarity of the provided GIS and data packages, which is promising for a future use as training tools. Most PIs report positive involvement and motivation from their operators. Each team had two multi-operator meetings, with about 3-10 people attending. The size of the team was ideal for a such exercise, more people would have been challenging to have good discussions. In some cases, the digital meetings have been complemented with complementary modes of communication (email discussions, sharing of comments in documents, prints screens, powerpoints, sending recording of meetings). The discussion at the meetings (and through other communication modes) were found very valuable; both for personal learning purpose and for improving the quality of the final products. Having operators with different skills and backgrounds brings value to the results. All involved institutions and PIs agree that the combination of different points of view and experiences from several regions around the World ensures that various morpho-kinematic elements are identified and taken into consideration. Although InSAR interpretation has been identified as the most challenging step due to little experience for some operators, several teams report that the data is useful at different levels, e.g. simply to detect landforms that may not be so obvious on optical images only, even when not focusing on quantifying their movement rates.

The analysis of the current CRDP (v.1.1) highlighted the value of the datasets for various usage: further detailed analysis in the considered area, selection of landforms for RGV generation, training dataset for machine learning, dissemination as online exercise for educational purpose. Several limitations and suggestions to improve the current procedure/guidelines have also been identified and are detailed in the PVIR [RD-11] and PUG [RD-12]. These elements will be further discussed in the publication associated with the open release of the dataset (in prep., see Section 5).

In the second iteration, the results may be used as training data for RoGI using machine learning. This is planned to be performed by third parties, in synergy with an upcoming RGIK working group on the same topic. Based on the findings of the exercise, we will also encourage all partners institutions to correct their initial regional inventories (Permafrost_cci Phase 1). Identified sections of RGIK guidelines showing a lack of clarity will be adjusted based on the exercise conclusions. Based on the updated guidelines, we are planning the generation of inventories in new regions. Further support for external partners will be discussed at the end of iteration 1.

3.8 Assessment of utility of Rock Glacier Velocity (RGV) Products

Four different InSAR-RGV were produced at selected sites in the Swiss Alps [RD-10]. For the four sites, the relative velocity changes are homogenous. On average, the four rock glaciers all accelerated during the observation period, which matches both the trend shown by all UNIFR monitored rock glaciers in Valais and Central Swiss Alps and the trend from all rock glaciers monitored by the Swiss Permafrost Monitoring Network PERMOS [RD-11]. In general, all sites fit well with the trend documented by the regional and PERMOS averages. The results also match with the findings of Kellerer-Pirklbauer et al. (2024), who observed accelerating trends between 2018 and 2021 on multiple rock glaciers in the European Alps. Based on InSAR-RGV, all sites increase the most between 2018 and 2019, as for the PERMOS results (PERMOS, 2023).

In conclusion, the preliminary assessment of the Permafrost_cci RGV products show that the InSAR-RGV result from the iteration 1 Permafrost_cci Phase 2 are promising. We propose an easily transferable method to automate the production of RGV by averaging unwrapped Sentinel-1 interferograms. The developed method appears to be suitable to produce consistent InSAR-RGV, which are comparable to GNSS-RGV, although we need to include more years of data to confirm this primary conclusion. The InSAR-RGV products are an average of several pixels on the main moving areas of each rock glacier, providing a better spatial representativity than single GNSS points. In addition, because of the availability of historical data, time series can be computed since 2015 and 2017 with 6-days and 12-days interferograms, respectively, whereas in-situ measurements are only available from the first measurement onwards. As long as regular open access data is available, the RGV time series can updated each year.

There are several open questions regarding the operationalization of the InSAR-RGV production, as this part was designed as a pilot study in the first iteration. The generic RGV guidelines are still under development and advances in this field are highly expected in the coming years, under the umbrella of the RGIK community. The InSAR procedure applied at the Swiss pilot sites needs to be tested on many rock glaciers and the time series should be compared with other techniques (e.g. optical remote sensing). This will be the focus of the second iteration of Permafrost_cci Phase 2 and the Option 8 (PermaSeries: Integration of complementary rock glacier velocity time series for the monitoring of mountain permafrost). An international working group has recently been kicked-off to produce and intercompare RGV generated with different techniques (in situ, optical remote sensing, radar remote sensing) on similar selected rock glaciers. The kick-off meeting was organized the 10th of April 2024 and a dedicated workshop on this topic is planned in the Fall 2024.

In the long run, Permafrost_cci contributes to the objective to complement in-situ monitoring sites with a large set of remotely sensed RGV in more regions and on more landforms in each region. The effort of data collection and comparison has started (Pellet et al., 2023) but is recent and the analysis is currently based on few sites worldwide. Systematic generation using the Permafrost_cci InSAR-RGV methodology and further development of similar approaches for other remote sensing techniques will contribute to enlarge the set of comparable RGVs. Further analyse in respect to climate variables and other ECV products (PT, ALT) in similar regions will allow for comprehensive evaluation of the RGV significance as climate change indicator.

4 Progress in regard to user requirements

4.1 Algorithm selection

The process of the algorithm selection as detailed in the User Requirements Documents (URD) [RD-4,7] has been driven by the requirements of the climate research community. The user community deemed the selected algorithm as appropriate for their applications.

4.2 Product specification

In Table 4, we specify user requirements from the URD [RD-4] for the CryoGrid products and show the respective status of achievement. We aimed to complete as many requirements as possible, which are marked in green. Table 5 addresses the rock glacier product requirements.

Table 4: Summary of user requirements. Background (BG) means that this is a continuous activity, production (P), and dissemination (D) means that the related requirement has to be considered during production, and dissemination, respectively. Parameters are Permafrost Extent (PE), Ground Temperature (GT) and Active Layer Thickness (ALT). The last column indicates the achievement status for the fourth project year (Y4=year 4; red: not started, yellow: ongoing, green: completed).

ID	Parameter	Requirements	Source	Type	Y4
URQ_01	PE/GT/ALT	higher spatial resolution than a map scale of 1:10,000,000	IPA Mapping group report	BG	green
URQ_02	PE/GT/ALT	data need to be related to a time stamp	IPA Mapping group report	P	green
URQ_03	PE/GT/ALT	form of delivery for maps and data need to be flexible	IPA Mapping group report	D	green
URQ_04	PE/GT/ALT	high data quality	IPA Mapping group report	BG	yellow
URQ_05	PE/GT/ALT	benchmark dataset needs to be developed	IPA Mapping group report, GlobPermafrost/IPA mapping group workshop	P	green
URQ_06	PE/GT/ALT	evaluation through community	GlobPermafrost/IPA mapping group workshop	P	green
URQ_07	PE/GT/ALT	terminology for modelling output 'potential'	GlobPermafrost/IPA mapping group workshop	D	green
URQ_08	GT/ALT	depth of active layer, permafrost temperature in	GCOS	BG	green

		K and seasonal soil freeze/thaw needs to be addressed			
URQ_09	PE	Threshold: uncertainty 10-25%, hor. res. 10-100 km, temp. res. 3-5 days, timeliness 5-6 days;	OSCAR	BG	
		breakthrough uncertainty 7-8.5%, hor. res. 0.85 - 1 km, temp. res. 14-36 hours, timeliness 14-36 h			
URQ_10	PE/GT/ALT	Distribution as NetCDF	CMUG	D	
URQ_11	PE/GT/ALT	Development of a new ground stratigraphy product for the permafrost domain	GlobPermafrost survey	P/D	
URQ_12	GT	Threshold: pan-arctic, yearly, last decade, 10km, RMSE<2.5°C,	Permafrost_cci survey	BG	
		Target, global, monthly, 1979- present, 1km, subgrid variability, RMSE < 0.5°C			
URQ_13	ALT	Threshold: pan-arctic, yearly, last decade, 10km, RMSE<25cm, Target, global, monthly, 1979- present, 1km, subgrid variability, RMSE<10cm	Permafrost_cci survey	BG	

Table 5. *Summary of user requirements for the Rock Glacier Inventories (RoGI) and the Rock Glacier Velocity (RGV) products [RD-7]. In the column 'Type', Background (BG) means that the requirement relates to the initial selection of the study areas, data and/or methods. Production (P) means that the related requirements must be considered during the production phase. Evaluation (E) means that the requirements are related to the quality assessment of the products. The colours show the achievement status at the end of the Phase II iteration 1 (in black:* ***Threshold Requirement****; in blue:* ***Breakthrough Requirement****; in green:* ***Goal Requirement****). ***Note that no Breakthrough Requirement was initially defined for URq_03 but the products reached an intermediate level between Threshold and Goal, corresponding to a Breakthrough level. The last column indicates the achievement status for the fourth project year (Y4=year 4; red: not started, yellow: ongoing, green: completed).*

ID	PARAMETER	USER REQUIREMENTS	TYPE	Y4
URq_01	RoGI	Relevant geographical coverage at the local-regional scale (valley side, drainage basin, mountain range).	BG	green
URq_02	RoGI	Inventory based on several recent datasets over the 5-10 past years.	BG	green
URq_03 ***	RoGI	Identification by a primary marker (point) and rock glacier outline as a polygon following the extended and/or restricted geomorphological footprints).	P	green
URq_04	RoGI	Differentiation of rock glacier units (RGU) and mono-unit or multi-unit systems (RGS), based on distinct timing of formation, different connections to the upslope unit or distinct activities/kinematics.	P	yellow
URq_05	RoGI	Mandatory documentation of the temporal properties (acquisition data, time frame/window) of the data sources used for RoGI generation, required for comparison and potential future update.	P/E	yellow
URq_06	RoGI	Updated activity categorization: active, transitional, or relict. Uncertainty between categories can be documented.	P	green
URq_07	RoGI	Optional destabilization attribute, only documented when geomorphological or kinematic evidence is available.	BG/P	yellow
URq_08	RoGI	Semi-quantitative velocity classes, depending on the applied technique: For InSAR: 1-3 cm/yr, 3-10 cm/yr, 10-30 cm/yr, 30-100 cm/yr, etc.	BG/P	green
URq_09	RoGI	Semi-quantitative 'half an order-of-magnitude' categories: cm-dm/yr, dm/yr, dm-m/yr, m/yr, etc.	P	green

URq_10	RoGI	The data properties (data source, dimensionality, time window/frame) must be documented for all attributes. The reliability and spatial representativeness of moving areas and kinematic attributes must be qualitatively assessed (low, medium, high).	P/E	
URq_11	RGV	Multiple sites in a defined region, allowing for preliminary analysis of similar/dissimilar trends.	BG	
URq_12	RGV	Active or transitional rock glaciers with movement related to permafrost creep. Sites where long-term monitoring is feasible. Rock glacier units fully characterised following RoGI requirements.	BG	
URq_13	RGV	1 year, i.e. measured or computed once a year.	BG/P	
URq_14	RGV	Observation time window < 1 year (e.g. summer period only). At least 1 month and consistent over time (max. ≈15 days of difference).	BG/P	
URq_15	RGV	Temporal extent: past 5-10 years	BG/P	
URq_16	RGV	Annual mean velocity value. Unit: m/yr	P	
URq_17	RGV	The velocity is aggregated from flow field or several discrete points covering a large part of the rock glacier unit. The aggregation procedure and the considered area should be consistent over time.	P	
URq_18	RGV	Maximal relative error of the velocity data: 20%. If the error exceeds 20%, the site must be discarded, or alternative techniques should be considered in accordance with the absolute velocity measured/computed of the selected rock glacier.	E	
URq_19	RGV	The RGV consistency needs to be ensured.	E	

4.3 Plan for operationalization of PE, GT and ALT

The ESA Permafrost_cci processing chain is currently implemented on the network of Norwegian supercomputing clusters managed by the company Sigma2 (www.sigma2.no). In principle, operational services for Permafrost ECV generation could be conducted as-is on the Sigma2 infrastructure, although significantly higher rates may be charged for both CPU hours and storage for commercial users than for universities and research institutes. Furthermore, the processing chain is partly implemented in Matlab, so that access to licenses could become a cost factor or even a limitation, especially for commercial entities. In the following, we summarize principal requirements for an operational processing system, as well as changes to the processing chain that have been or should ideally be implemented to achieve operational services.

Constraints on current processing system: Hardware: supercomputing cluster with at least 100 cores with 4GB fast memory per core, about 15 TB storage for input data sets. Software: Matlab; slurm for management of supercomputing cluster.

Steps already implemented towards operationalization: In the year 1 to 3 processing, only the ECV parameters are stored, e.g. annual averages of ground temperatures. In order to compute a new time slice (e.g. another year), the entire processing for all previous years must be repeated, as it was not possible to store the "raw" model state due to memory limitations. In the year 4 processing in Permafrost_cci, the possibility to restart simulations from the raw model state at a particular point in time has been implemented. In particular, this makes it possible to compute, update and continue an existing ECV time series when new EO data become available. We estimate that this reduces the amount of computation by about a factor of 50 compared to recomputing the entire time period, which makes operational releases of the Permafrost_cci ECV products much more feasible.

Further changes to the processing system that will make operationalization easier: While there is no principal problem using the Matlab processing language for processing, it may introduce complications and potentially costs for operational entities. Recoding the processing chain in an open-source language would therefore be desirable, but the complexity of the processing chain makes this re-coding difficult and potentially costly. Recoding in C++ is the most feasible option as there is an automatic C++ code converter available in Matlab. At present, not all code structures required for the processing system are supported, in particular recursive data structures of objects like linked lists. However, the capabilities of the code converter have steadily improved from year to year: in particular, in the 2024a version of Matlab, code containing arrays of objects can for the first time be automatically converted C++ code, which in previous versions was a key shortcoming of the automatic code conversion. We expect support for recursive data structures in the coming years which would strongly reduce the working time and thus the costs required to re-implement the Permafrost_cci processing chain in C++. We emphasize that changes to the processing system are much easier to implement in the current Matlab-based processing chain which is specially designed for modularity. Therefore, unless fast automatic code conversion becomes fully available, re-coding of the processing system in C++ or other languages should only be commenced when the processing system is fully consolidated.

5 Publications and outreach

5.1 Publications

Peer-reviewed scientific articles

Accepted/Published

Aga, J., Boike, J., Langer, M., Ingeman-Nielsen, T., and Westermann, S.: Simulating ice segregation and thaw consolidation in permafrost environments with the CryoGrid community model, The Cryosphere, 17, 4179–4206, https://doi.org/10.5194/tc-17-4179-2023, 2023.

Ardelean, F.; Onaca, A.; Chețan, M.-A.; Dornik, A.; Georgievski, G.; Hagemann, S.; Timofte, F.; Berzescu, O. (2020). Assessment of Spatio-Temporal Landscape Changes from VHR Images in Three Different Permafrost Areas in the Western Russian Arctic. Remote Sensing. 12(23), 3999. https://doi.org/10.3390/rs12233999

Bartsch, A., Ley, S., Nitze, I., Pointner, G., & Vieira, G. (2020). Feasibility study for the application of Synthetic Aperture Radar for coastal erosion rate quantification across the Arctic. Frontiers in Environmental Science, 8(143). https://doi.org/10.3389/fenvs.2020.00143

Bartsch,, A. G. Pointner, H. Bergstedt, B. Widhalm, A. Wendleder, A. Roth (2021). Utility of polarizations available from Sentinel- 1 for tundra mapping. IGARSS 2021 proceedings.

Bartsch, A., Strozzi, T., & Nitze, I. (2023). Permafrost Monitoring from Space. Surveys in Geophysics, 44(5), 1579–1613. https://doi.org/10.1007/s10712-023-09770-3

Bergstedt, H., Bartsch, A., Neureiter, A., Höfler, A., Widhalm, B., Pepin, N., and Hjort, J. (2020). Deriving a Frozen Area Fraction From Metop ASCAT Backscatter Based on Sentinel-1. IEEE Transactions on Geoscience and Remote Sensing, Volume: 58, Issue: 9. https://doi.org/10.1109/TGRS.2020.2967364

Bergstedt, H., Bartsch, A., Duguay, C. R., & Jones, B. M. (2020). Influence of surface water on coarse resolution C-band backscatter: Implications for freeze/thaw retrieval from scatterometer data. Remote Sensing of Environment, 247, 111911. https://doi.org/10.1016/j.rse.2020.111911

Bertone A, Jones N, Mair V, Scotti R, Strozzi T, Brardinoni F. In press (Accepted on March 20, 2024). A climate-driven, altitudinal transition in rock glacier dynamics detected through integration of geomorphologic mapping and InSAR-based kinematic information. The Cryosphere. https://tc.copernicus.org/preprints/tc-2023-143/

Bertone, A., Barboux, C., Bodin, X., Bolch, T., Brardinoni, F., Caduff, R., Christiansen, H. H., Darrow, M., Delaloye, R., Etzelmüller, B., Humlum, O., Lambiel, C., Lilleøren, K. S., Mair, V., Pellegrinon, G., Rouyet, L., Ruiz, L., and Strozzi, T. 2022. Incorporating InSAR kinematics into rock glacier inventories: insights from 11 regions worldwide, The Cryosphere, 16, 2769–2792. https://doi.org/10.5194/tc-16-2769-2022.

Brouillette, M.: How microbes in permafrost could trigger a massive carbon bomb. Nature, 591, 360-362 (2021) on 17 March 2021. https://www.nature.com/articles/d41586-021-00659-y

Biskaborn, B. K.; Smith, S. L.; Noetzli, J.; Matthes, H.; Vieira, G.; Streletskiy, D. A.; Schoeneich, P.; Romanovsky, V. E.; Lewkowicz, A. G.; Abramov, A.; Allard, M.; Boike, J.; Cable, W. L.; Christiansen, H. H.; Delaloye, R.; Diekmann, B.; Drozdov, D.; Etzelmüller, B.; Grosse, G.; Guglielmin, M.; Ingeman-Nielsen, T.; Isaksen, K.; Ishikawa, M.; Johansson, M.; Johannsson, H.; Joo, A.; Kaverin, D.; Kholodov, A.; Konstantinov, P.; Kröger, T.; Lambiel, C.; Lanckman, J.-P.; Luo, D.; Malkova, G.; Meiklejohn, I.; Moskalenko, N.; Oliva, M.; Phillips, M.; Ramos, M.; Sannel, A. B. K.; Sergeev, D.; Seybold, C.; Skryabin, P.; Vasiliev, A.; Wu, Q.; Yoshikawa, K.; Zheleznyak, M., Lantuit, H. (2019): Permafrost is warming at a global scale. Nature Communications, 10, 264. https://doi.org/10.1038/s41467-018-08240-4

Biskaborn, B. K., Lanckman, J.-P., Lantuit, H., Elger, K., Streletskiy, D. A., Cable, W. L., and Romanovsky, V. E. (2015): The new database of the Global Terrestrial Network for Permafrost (GTN-P). Earth Syst. Sci. Data, 7, 245–259. https://doi.org/10.5194/essd-7-245-2015

Burke, E. J., Zhang, Y., & Krinner, G. (2020). Evaluating permafrost physics in the Coupled Model Intercomparison Project 6 (CMIP6) models and their sensitivity to climate change. The Cryosphere, 14(9), 3155–3174. https://doi.org/10.5194/tc-14-3155-2020

Jones, B. M. , Arp, C. D. , Grosse, G. , Nitze, I. , Lara, M. J., Whitman, M. S. , Farquharson, L. M. , Kanevskiy, M. , Parsekian, A. D. , Breen, A. L. , Ohara, N. , Rangel, R. C. and Hinkel, K. M. (2020): Identifying historical and future potential lake drainage events on the western Arctic coastal plain of Alaska. Permafrost and Periglacial Processes, 31 (1), 110-127. https://doi.org/10.1002/ppp.2038

Jones, B. M., Schaeffer Tessier, S., Tessier, T., Brubaker, M., Brook, M., Schaeffer, J., Ward Jones, M. K., Grosse, G., Nitze, I., Rettelbach, T., Zavoico, S., Clark, J. A., & Tape, K. D. (2023). Integrating local environmental observations and remote sensing to better understand the life cycle of a thermokarst lake in Arctic Alaska. Arctic, Antarctic, and Alpine Research, 55(1), 2195518. https://doi.org/10.1080/15230430.2023.2195518

Jones, B. M., Irrgang, A. M., Farquharson, L. M., Lantuit, H., Whalen, D., Ogorodov, S., Grigoriev, M., Tweedie, C., Gibbs, A. E., Strzelecki, M. C., Baranskaya, A., Belova, N., Sinitsyn, A., Kroon, A., Maslakov, A., Vieira, G., Grosse, G., Overduin, P., Nitze, I., Maio, C., Overbeck, J., Bendixen, M., Zagórski, P., Romanovsky, V.E. (2020). NOAA Arctic Report Card 2020, Coastal Permafrost Erosion, Administrative Report. https://doi.org/10.25923/E47W-DW52

Kääb, A., Strozzi, T., Bolch, T., Caduff, R., Trefall, H., Stoffel, M., & Kokarev, A. (2021). Inventory and changes of rock glacier creep speeds in Ile Alatau and Kungöy Ala-Too, northern Tien Shan, since the 1950s. The Cryosphere, 15(2), 927–949. https://doi.org/10.5194/tc-15-927-2021

Lambiel, C., Strozzi, T., Paillex, N., Vivero, S. and Jones, N. 2023. Inventory and kinematics of active and transitional rock glaciers in the Southern Alps of New Zealand from Sentinel-1 InSAR, Arctic, Antarctic, and Alpine Research, 55(1), 2183999. https://doi.org/10.1080/15230430.2023.2183999.

Langer, M., von Deimling, T.S., Westermann, S., Rolph, R., Rutte, R., Antonova, S., Rachold, V., Schultz, M., Oehme A., Grosse G. Thawing permafrost poses environmental threat to thousands of sites with legacy industrial contamination. Nat Commun 14, 1721 (2023). https://doi.org/10.1038/s41467-023-37276-4.

Lenton, T.M., Abrams, J.F., Bartsch, A. et al. Remotely sensing potential climate change tipping points across scales. Nat Commun 15, 343 (2024). https://doi.org/10.1038/s41467-023-44609-w.

Lilleøren, K. S., Etzelmüller, B., Rouyet, L., Eiken, T., Slinde, G., and Hilbich, C.: Transitional rock glaciers at sea level in northern Norway, Earth Surf. Dynam., 10, 975–996, 2022. https://doi.org/10.5194/esurf-10-975-2022.

Lissak, C., Bartsch, A., De Michele, M., Gomez, C., Maquaire, O., Raucoules, D., & Roulland, T. (2020). Remote Sensing for Assessing Landslides and Associated Hazards. Surveys in Geophysics, 41(6), 1391–1435. https://doi.org/10.1007/s10712-020-09609-1

Martin, L. C. P., Nitzbon, J., Scheer, J., Aas, K.S., Eiken, T., Langer, M., Filhol, S., Etzelmüller, B., & Westermann, S. (2021). Lateral thermokarst patterns in permafrost peat plateaus in northern Norway. The Cryosphere, 15, 3423–3442. https://doi.org/10.5194/tc-15-3423-2021

Nitze, I., Cooley, S. W., Duguay, C. R., Jones, B. M., & Grosse, G. (2020). The catastrophic thermokarst lake drainage events of 2018 in northwestern Alaska: Fast-forward into the future. The Cryosphere, 14(12), 4279–4297. https://doi.org/10.5194/tc-14-4279-2020

Nitze, I., Heidler, K., Barth, S., & Grosse, G. (2021). Developing and Testing a Deep Learning Approach for Mapping Retrogressive Thaw Slumps. Remote Sensing, 13(21). https://doi.org/10.3390/rs13214294

Obu, J. (2021). How Much of the Earth's Surface is Underlain by Permafrost? Journal of Geophysical Research: Earth Surface, 126(5). https://doi.org/10.1029/2021JF006123

Pellet, C., Bodin, X., Cusicanqui, D., Delaloye, R., Kaufmann, V., Noetzli, J., Thibert, E., Vivero, S., & Kellerer-Pirklbauer, A. 2023. Rock glacier velocity. In State of Climate 2022 (Vol. 104, pp. 41–42). https://doi.org/10.1175/2023BAMSStateoftheClimate.1.

Popp, T., M.I. Hegglin, R. Hollmann, F. Ardhuin, A. Bartsch, A. Bastos, V. Bennett, J. Boutin, C. Brockmann, M. Buchwitz, E. Chuvieco, P. Ciais, W. Dorigo, D. Ghent, R. Jones, T. Lavergne, C.J. Merchant, B. Meyssignac, F. Paul, S. Quegan, S. Sathyendranath, T. Scanlon, M. Schröder, S.G.H. Simis, U. Willén (2020): Consistency of satellite climate data records for Earth system monitoring. Bulletin of the American Meteorological Society. https://doi.org/10.1175/BAMS-D-19-0127.1

Renette, C., Aalstad, K., Aga, J., Zweigel, R. B., Etzelmüller, B., Lilleøren, K. S., Isaksen, K., and Westermann, S.: Simulating the effect of subsurface drainage on the thermal regime and ground ice in blocky terrain in Norway, Earth Surf. Dynam., 11, 33–50, https://doi.org/10.5194/esurf-11-33-2023, 2023.

Rouyet, L., Lilleøren, K.S., Böhme, M., Vick, L.M., Delaloye, R., Etzelmüller, B., Lauknes, T.R., Larsen, Y., and Blikra, L.H. 2021. Regional Morpho-Kinematic Inventory of Slope Movements in Northern Norway, Front. Earth Sci. 9, 6810881. https://doi.org/10.3389/feart.2021.681088.

Rouyet, L., Liu, L., Strand, S. M., Christiansen, H. H., Lauknes, T. R., & Larsen, Y. (2021). Seasonal InSAR Displacements Documenting the Active Layer Freeze and Thaw Progression in Central-Western Spitsbergen, Svalbard. Remote Sensing, 13(15), 2977. https://doi.org/10.3390/rs13152977

Runge, A. and Grosse, G. (2020): Mosaicking Landsat and Sentinel-2 Data to Enhance LandTrendr Time Series Analysis in Northern High Latitude Permafrost Regions. Remote Sensing, 12(15), 2471. https://doi.org/10.3390/rs12152471

Runge, A., Nitze, I., & Grosse, G. (2022). Remote sensing annual dynamics of rapid permafrost thaw disturbances with LandTrendr. Remote Sensing of Environment, 268, 112752. https://doi.org/10.1016/j.rse.2021.112752

Strauss, J., Fuchs, M., Hugelius, G., Miesner, F., Nitze, I., Opfergelt, S., Schuur, E., Treat, C., Turetsky, M., Yang, Y., & Grosse, G. (2024). Organic matter storage and vulnerability in the permafrost domain. In Reference Module in Earth Systems and Environmental Sciences (p. B9780323999311001641). Elsevier. https://doi.org/10.1016/B978-0-323-99931-1.00164-1

Strozzi T., R.Caduff, N. Jones, C. Barboux, R, Delaloye, X. Bodin, A. Kääb, E. Mätzler, L. Schrott (2020). Monitoring Rock Glacier Kinematics with Synthetic Aperture Radar. Remote Sensing, 12(3), 559. https://doi.org/10.3390/rs12030559

Swingedouw, D., Speranza, C., Bartsch, A., Durand, G., Jamet, C., Beaugrand, G., Conversi, A. (2020): Early Warning from Space for a Few Key Tipping Points in Physical, Biological, and Social-Ecological Systems. Surveys in Geophysics. https://doi.org/10.1007/s10712-020-09604-6

Tape, K. D., Clark, J. A., Jones, B. M., Kantner, S., Gaglioti, B. V., Grosse, G., & Nitze, I. (2022). Expanding beaver pond distribution in Arctic Alaska, 1949 to 2019. Scientific Reports, 12(1), 7123. https://doi.org/10.1038/s41598-022-09330-6

Veremeeva, A., Nitze, I., Günther, F., Grosse, G., & Rivkina, E. (2021). Geomorphological and Climatic Drivers of Thermokarst Lake Area Increase Trend (1999–2018) in the Kolyma Lowland Yedoma Region, North-Eastern Siberia. Remote Sensing, 13(2), 178. https://doi.org/10.3390/rs13020178

Westermann, S., Ingeman-Nielsen, T., Scheer, J., Aalstad, K., Aga, J., Chaudhary, N., Etzelmüller, B., Filhol, S., Kääb, A., Renette, C., Schmidt, L. S., Schuler, T. V., Zweigel, R. B., Martin, L., Morard, S., Ben-Asher, M., Angelopoulos, M., Boike, J., Groenke, B., Miesner, F., Nitzbon, J., Overduin, P., Stuenzi, S. M., and Langer, M.: The CryoGrid community model (version 1.0) – a multi-physics toolbox for climate-driven simulations in the terrestrial cryosphere, Geosci. Model Dev., 16, 2607–2647, https://doi.org/10.5194/gmd-16-2607-2023, 2023.

Wolter, J., Jones, B. M., Fuchs, M., Breen, A. L., Bussmann, I., Koch, B. P., Lenz, J., Myers-Smith, I. H., Sachs, T., Strauss, J., Nitze, I., & Grosse, G. (2024). Post-drainage vegetation, microtopography and organic matter in Arctic drained lake basins. Environmental Research Letters. https://doi.org/10.1088/1748-9326/ad2eeb

Yang, Y., Rogers, B. M., Fiske, G., Watts, J., Potter, S., Windholz, T., Mullen, A., Nitze, I., & Natali, S. M. (2023). Mapping retrogressive thaw slumps using deep neural networks. Remote Sensing of Environment, 288, 113495. https://doi.org/10.1016/j.rse.2023.113495

In prep./Submitted/In review/In revision

Heidler, K., Nitze, I., Grosse, G., & Zhu, X. X. (2024). PixelDINO: Semi-Supervised Semantic Segmentation for Detecting Permafrost Disturbances (arXiv:2401.09271). arXiv. http://arxiv.org/abs/2401.09271

Hu, Y., Arenson, L.U., Barboux, C., Bodin, X., Cicoira, A., Delaloye, R., Gärtner-Roer I., Kääb, A., Kellerer-Pirklbauer, A., Lambiel, C., Liu, L., Pellet, C., Rouyet, L, Schoeneich, P., Seier, G. Rock Glacier Velocity as a new product of Essential Climate Variable for Permafrost. In prep.

Nitze, I., Van Der Sluijs, J., Barth, S., Bernhard, P., Huang, L., Lara, M., Kizyakov, A., Runge, A., Veremeeva, A., Ward Jones, M., Witharana, C., Xia, Z., & Liljedahl, A. (2024). A labeling intercomparison of retrogressive thaw slumps by a diverse group of domain experts. https://doi.org/10.31223/X55M4P

Rouyet, L., Delaloye, R., Bolch, T., Brardinoni, F., Caduff, R., Cusicanqui, D., Darrow, M., Echelard, T., Lambiel, T., Lambiel, C., Ruiz, L., Sirbu, F., Strozzi, T. Rock Glacier Inventories (RoGI) in 12 areas worldwide using a multi-operator mapping procedure. In prep.

Vivero, S. Brardinoni, F., Bodin, X., Delaloye, R., Lambiel, C., MacDonnell, S., Ruiz, L., Rouyet, L., Cicoira, A., Hu, Y., Wehbe, M., Schaffer, N. The RGIK initiative: recommendations for inventorying and mapping rock glaciers worldwide. In prep.

Zwieback, S., Liu, L., Rouyet, L., Short, N., Strozzi, T. Advances in InSAR analysis of permafrost terrain. Submitted. Permafrost and Periglacial Processes.

Community guidelines and white papers

RGIK, 2023. Puigcerdà Commitment. IPA Action Group Rock glacier inventories and kinematics. 4 pp. https://www.rgik.org.

RGIK. 2023. Guidelines for inventorying rock glaciers: baseline and practical concepts (version 1.0). IPA Action Group Rock glacier inventories and kinematics, 25 pp. https://doi.org/10.51363/unifr.srr.2023.002.

RGIK. 2022. Optional kinematic attribute in standardized rock glacier inventories (version 3.0.1). IPA Action Group Rock glacier inventories and kinematics, 8 pp. https://www.rgik.org.

RGIK. 2023. InSAR-based kinematic attribute in rock glacier inventories. Practical InSAR guidelines (version 4.0). IPA Action Group Rock glacier inventories and kinematics, 33 pp. https://www.rgik.org.

RGIK 2023. Rock Glacier Velocity as an associated parameter of ECV Permafrost: baseline concepts (version 3.2). IPA Action Group Rock glacier inventories and kinematics, 12 pp. https://www.rgik.org.

RGIK. 2023. Rock Glacier Velocity as an associated parameter of ECV Permafrost: practical concepts (version 1.2). IPA Action Group Rock glacier inventories and kinematics, 17 pp. https://www.rgik.org.

RGIK. 2023. Instructions of the RoGI exercises in the Goms and the Matter Valley (Switzerland). IPA Action Group Rock glacier inventories and kinematics, 10 pp. https://www.rgik.org.

5.2 News Stories

February 25 .2020 ESA – Picturing permafrost in the Arctic
http://www.esa.int/Applications/Observing_the_Earth/Space_for_our_climate/Picturing_permafrost_in_the_Arctic

March 4, 2020. H2020 Nunataryuk
https://nunataryuk.org/news/139-new-map-shows-extent-of-permafrost-in-northern-hemisphere

Cover image of Permafrost and Periglacial Processes, volume 31, issue 3, July-September 2020, shows new permafrost map produced by UNEP Grid Arendal based on submarine permafrost map by Overduin et al. 2019 and land-based permafrost by Obu et al. 2019.

2022 IPA: Frozen Ground 43, the News Bulletin of the IPA,
https://www.permafrost.org/frozen-ground-newsletter/

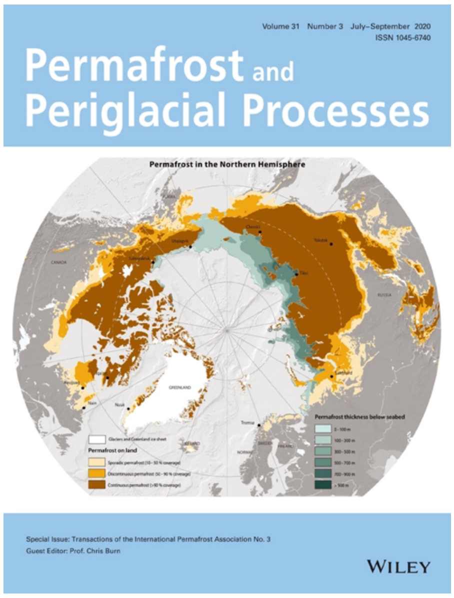

April 19, 2023: ESA - Permafrost Monitoring from Space – a review: Understanding the implications of thawing permafrost is expected to advance with enhanced data availability and products, https://climate.esa.int/en/news-events/permafrost-monitoring-from-space-a-review

12/12/2023: Permafrost thaw: a silent menace, ESA - European Space Agency,
https://www.esa.int/ESA_Multimedia/Videos/2023/12/Permafrost_thaw_a_silent_menace

5.3 User workshops

The first Permafrost_cci user workshop took place on September 27th 2021. It was held online with 66 participants. The project status was presented first. The first block of user presentations comprised climate modelling topics. The project use case #1 (HIRHAM) was presented by Heidrun Matthes (section 3.2). Kazuyuki Saito (YAMSTEC) discussed issues regarding soil organic carbon and ground ice dynamics in climate models. Eleanor Burke (Metoffice) showed a detailed assessment of permafrost_cci records with respect to CMIP6 activities. Ground temperature trends are similar to past records. This block was followed by planned and ongoing activities which combine or compare to other satellite products. This included an ESA fellowship presentation (A. Runge , AWI), use case #2 (Ingmar Nitze, AWI; section 3.3) and status of RECCAP-2 (Gustaf Hugelius, University Stockholm). The last user presentation block referred to applications of the permafrost extent product of DUE GlobPermafrost. Eventually, challenges in production and validation have been presented by Permafrost_cci team members. This covered lowland and mountain permafrost. The importance of validation in mountain areas and associated issues have been discussed. The need for documentation of how to work with the Polar Stereographic projection in GIS environment has been pointed out. In general there was positive feedback regarding the availability as NetCDF. The final discussion specifically addressed climate modelling applications. The following requirements have been stated:

- Monthly timesteps
- High vertical resolution (also 20 and 50 cm)
- Recommendations for aggregation/resampling to modelling grids

Rock glacier products:

- RGIK user workshop, 17 June 2023, Puigcerdà, Spain. Approx. 45 attendees.
- Upcoming: RGV workshop, 20–22 November 2024, Fribourg, Switzerland.

5.4 Outreach activities

Option 6 results were presented as a *Webinar of the Permafrost Discovery Gateway*, 5th of October 2023: Bartsch, A. 'The Arctic land north of the treeline at 10m' https://arcticdata.io/catalog/portals/permafrost/Stay-Connected (recording published on youtube: https://www.youtube.com/watch?v=xGGrLoUJlxk)

The *Arctic Permafrost Atlas* from the Nunataryuk project, which contains permafrost_cci output on several pages (e.g., 47 and 91), was released: https://gridarendal-website-live.s3.amazonaws.com/production/documents/:s_document/1041/original/PermafrostAtlas_20oct_finaldraft.pdf?1697708753

Permafrost_cci results were presented at the 13th *CCI colocation and CMUG Integration meetings*, which took place between November 7 and 9, 2023 at the ESA ECSAT conference centre in Harwell (Oxfordshire, UK).

A presentation on "The potential and limitations of remote sensing for the ECV Permafrost" was held at the *ISSI Workshop on Remote Sensing in Climatology* – ECVs and their Uncertainties, 13-17 November 2023.

A presentation on "Satellite data use for permafrost related monitoring in ESA and H2020 projects" was held at the *EC-ESA Joint Earth System Science Initiative*, 22-24 November 2023.

The project status has been further presented at

- as part of an invited talk at the Canadian Permafrost Day on the 1st of March 2023 (Bartsch et al.)
- as part of an invited talk at Arctic International Technical Conference (AITC 2023) Mapping the Arctic in Nuuk (Greenland), April 24-27 2023 (Strozzi et al.).
- the IPA Austria workshop on 28th of September 2023 (Mallnitz, Austria). (Bartsch et al.)

A presentation on "Tracking permafrost landscape dynamics in a rapidly warming Arctic" was held by Ingmar Nitze in the AI for Good webinar series. 28 February 2024

Rock glaciers:

- EGU RGIK splitter meeting, 15 April 2024. Approx. 25 attendees.
- Upcoming: ICOP RGIK side meeting, 17 June 2024, Whitehorse, Canada.

5.5 Presentations at scientific conferences (Phase II)

Past contributions

6th European Conference on Permafrost (EUCOP), 18–22 June 2023, Puigcerdà, Spain

A. Bartsch, T. Strozzi, I. Nitze. Permafrost Monitoring from Space – What Have We Learned So Far?

H. Bergstedt, A. L. Breen, B. M. Jones, L. Farquharson, J. Wolter, G. Grosse, A. Bartsch, M. Kanevskiy, C. von Baeckmann, T. Kumpula, A. Veremeeva, G. Hugelius, K. Ermokhina. Drained Lake Basins on a Panarctic Scale.

F. Brardinoni, A. Bertone, N. Jones, V. Mair, R. Scotti, T. Strozzi. A Rock Glacier Inventory Integrating Geomorphological Mapping and Sentinel-1 Satellite SAR Interferometry in Western South Tyrol, Italy.

T. Echelard, S. V. Andrade, L. Rouyet, C. Pellet, R. Delaloye, C. Barboux. Towards Practical Guidelines for Rock Glaciers Inventories (RoGI): A New 'User-friendly' GIS Tool for Training the Community.

A. Efimova, A. Bartsch, B. Widhalm, X. Muri, G. Hugelius, C. von Baeckmann. The Potential of High Resolution Landcover Classification as Proxy for Soil Properties.

K. Heidler, I. Nitze, G. Grosse, X. X. Zhu. Scaling Strategies for AI in Permafrost Remote Sensing.

B. Heim, M. Wieczorek, A. Irrgang, S. Lisovski, H. Matthes, G. Grosse, A. Haas, K. Elger, S. Westermann, C. Barboux, C. Pellet, R. Delaloye, F. M. Seifert, T. Strozzi, A. Bartsch. ESA CCI+ Permafrost - Validation Using International and National Permafrost Monitoring Networks.

A. Höhl, K. Heidler, A. Runge, G. Grosse, X. X. Zhu. Identifying and Interpreting Permafrost Vulnerability with Machine Learning.

Y. Hu, L. U. Arenson, C. Barboux, X. Bodin, A. Cicoira, R. Delaloye, I. Gärtner-Roer, A. Kääb, A. Kellerer-Pirklbauer, C. Lambiel, L. Liu, C. Pellet, L. Rouyet, P. Schoeneich, G. Seier, T. Strozzi. Rock Glacier Velocity as a New Product of the Essential Climate Variable Permafrost.

N. Jones, T. Strozzi, R. Caduff, F. Brardinoni, A. Bertone, L. Rouyet, L. Schmid, R. Delaloye. Rock Glacier Velocity in the Italian and Swiss Alps from Sentinel-1 Satellite SAR Interferometry.

T. Lübker, I. Nitze, S. Laboor, A. Irrgang, H. Lantuit, G. Grosse. A Web-based Portal for Serving Geospatial Information on Permafrost Disturbances to Permafrost Communities.

I. Nitze, M. J. Lara, G. Grosse. Continental-scale Drivers of Lake Drainage in Permafrost Regions.

A. Runge, A. Bartsch, A. Höhl, K. Heidler, B. Juhls, S. Westermann, G. Grosse. Identifying Linkages between EO-based Surface Variables and Permafrost Temperature Changes.

T. Strozzi, N. Jones, S. Westermann, A. Kääb, J. Boike, S. Antonova, A. Veremeeva, G. Grosse, A. Bartsch. Surface Deformation Monitoring of the Lena River Delta with Sentinel-1 SAR Interferometry.

A. Veremeeva, F. Guenther, T. Strozzi, A. Kizyakov, I. Nitze, C. Inauen, A. Morgenstern, N. Jones, M. Kanevskiy, A. Pismeniuk, M. Zimin, E. Rivkina, G. Grosse. Yedoma-alas Landscape Elevation Changes and Their Drivers Based on Sentinel-1 SAR Interferometry, Field Data, and High-resolution Optical Imagery, Bykovsky Peninsula, Laptev Sea Region.

A. Veremeeva, A. Morgenstern, S. Antonova, J. Boike, N. Bornemann, A. Cherepanova, M. Fuchs, M. Grigoriev, F. Guenther, A. Kizyakov, S. Laboor, F. Miesner, J. Nitzbon, E. Rivkina, A. Runge, L. Schirrmeister, U. Mathias, G. Grosse. Lena Delta Active Layer Thickness Database.

C. von Baeckmann, H. Bergstedt, A. Bartsch, B. Widhalm, A. Efimova, T. Kumpula, D. Ehrich, S. Abdulmanova, A. Sokolov. Land Cover Patterns for Drained Lake Basins across Bioclimatic Gradients.

S. Westermann, T. Ingeman-Nielsen, K. Aalstad, J. Aga, R. Zweigel, C. Willmes, L. Schmidt, B. Etzelmüller, A. Kääb, T. V. Schuler, C. Renette, L. Martin, S. Morard, M. Ben-Asher, J. Baptista, A. Bartsch, T. Strozzi, J. Boike, F. Miesner, J. Nitzbon, P. Overduin, S. Stuenzi, M. Langer. The CryoGrid Community Model - A Multi-physics Toolbox for Climate-driven Simulations in the Terrestrial Cryosphere.

B. Widhalm, A. Bartsch, T. Strozzi, N. Jones, M. Goeckede, M. Leibman, A. Khomutov, E. Babkina, E. Babkin. InSAR Application for Surface Displacement Investigations in Arctic Permafrost Regions: A Comparison of Mitigation Methods for Interfering Atmospheric Effects.

Cryosphere 2022 International Symposium on Ice, Snow and Water in a Warming World, 21–26 August 2022, Reykjavík, Iceland

Rouyet, L., Lauknes, T.R., Lilleøren, K.S., Etzelmüller, B., Kääb, A.M., Christiansen, H.H., Humlum, O., Delaloye, R., Strozzi, T., Bertone, A. 2022. SAR satellite remote sensing for mapping and monitoring Norwegian rock glaciers.

AGU 2023

Bartsch, Annett, Gustaf Hugelius, Barbara Widhalm, Aleksandra Efimova, Helena Bergstedt, Guido Grosse, Joshua Hashemi, Claire C Treat, Mathias Goeckede, Johanna Tamminen, Andreas Fix, Torsten Sachs, Sander Houweling, Dirk Schuettemeyer and AMPAC-Net Team. A51X-2297 Tackling Arctic landcover monitoring supporting The Arctic Methane and Permafrost Challenge (AMPAC) Network.

EGU 2024

- EGU24-8327, “Multi-annual Rock Glacier Velocity (RGV) products based on InSAR” by Lea Schmid et al., Posters on site in session GM10.5 - Interaction between climate, rock glaciers, andproglacial processes across scales.
- EGU24-15688, “Assessment of the Topographic Wetness Index in Permafrost landscapes” by Barbara Widhalm et al., Posters on site in session CR4.2 - Permafrost dynamics, interactions, feedbacks, disturbances and GHG's across scales: perspectives from observation to modelling.
- EGU24-16785, “Status of the Circumpolar Landcover Unit database” by Rustam Khairullin et al., Posters on site in session CR4.2 - Permafrost dynamics, interactions, feedbacks, disturbances and GHG's across scales: perspectives from observation to modelling.
- EGU24-14843, “Remote sensing supporting the Arctic Methane and Permafrost Challenge (AMPAC)” by Bartsch et al., Solicited presentation in US3 Bridging the scales: The Arctic methane and permafrost challenge
- The Rock Glacier Inventories and Kinematics (RGIK) initiative organized a splinter meeting (SPM66) at EGU24 on 15 April 2024 from 12:45 to 15:45 with the goal to provide a refresh on the current and planned RGIK activities as well as foster exchange and discussion between RGIK members.

Upcoming contributions

International Conference on Permafrost, 16-20 June 2024

I. Nitze, K. Heidler, K. Maier, S. Barth, A. Liljedahl, & G. Grosse. Using Deep Learning to Advance Global Monitoring of Retrogressive Thaw Slumps at High Spatio-Temporal Resolution.

K. Maier, P. Bernhard, I. Nitze, & I. Hajnsek. Automatic Segmentation Strategies for DEM-based RTS Monitoring.

C. Inauen, G. Grosse, M. Langer, I. Nitze, S. Barth, M. Baysinger, C. Hanna, T. Luebker, T. Rettelbach, A. Runge, & I. Hajnsek. Studying Drivers of Thermo-erosional Gully Development Based on In-situ Measurements, Remote Sensing Data, and Modeling.

K. Keskitalo, N. Speetjens, P. P. Overduin, S. Westermann, F. Miesner, T. Sachs, I. Nitze, L. Bröder, J. Lattaud, N. Haghipour, T. Eglinton, & J. Vonk. Landscape Characteristics and Particulate Organic Carbon Composition in the Peel River Watershed, Canada.

P. P. Overduin, B. Juhls, K. Keskitalo, I. Nitze, F. Miesner, N. Speetjens, J. Vonk, & S. Westermann. Hydrology of the Peel River, Yukon, Canada during the Extremely Dry Summer of 2019.

A. Bartsch, C. von Baeckmann, H. Bergstedt, B. Widhalm, B. Heim, M. Wieszorek, V. Döpper. 10m Resolution Circumpolar Landcover as Proxy for Permafrost Features.

F. Brardinoni, A. Bertone, V. Mair, N. Jones, T. Strozzi. Integrating Sentinel-1 and Cosmo-SkyMed InSAR-based Information for an Improved Regional Assessment of Rock Glacier Dynamics.

I. Gärtner-Roer, A. Kneib-Walter, A. Vieli, A. Cicoira, J. Beutel, T. Strozzi. Rockglacier Dynamics on Disko Island, Western Greenland.

C. Pellet, R. Delaloye, I. Gärtner-Roer, C. Lambiel, J. Noetzli, M. Phillips, C. Scapozza. On the Influence of Ground Surface Temperature on Rock Glacier Velocity.

L. Rouyet, R. Delaloye, T. Bolch, F. Brardinoni, R. Caduff, D. Cusicanqui, M. Darrow, T. Echelard, C. Lambiel, L. Ruiz, F. Sirbu, T. Strozzi. Multi-operator Mapping Exercise for Consensus-based Generation of Rock Glacier Inventories (RoGI) in 12 Areas Worldwide.

L. Schmid, L. Rouyet, R. Delaloye, C. Pellet, N. Jones, T. Strozzi. Multiannual Rock Glacier Velocity (RGV) Products Based on InSAR.

L. Wendt, L. Rouyet, H. H. Christiansen, S. Westermann. Evaluating InSAR Sensitivity to In-situ Ground Ice Contents Across Different Landforms.

S. Westermann, C. Willmes, L. Wendt, K. Aalstad, J. Aga, R. Zweigel, J. Røste, L. Rouyet, F. Miesner, B. Heim, M. Wieczorek, A. Kääb, B. Etzelmüller, T. Strozzi, A. Bartsch. Global-scale Mapping of Permafrost in a Changing Climate.

C. Willmes, S. Westermann, K. Aalstad. Improving Simulations of the Local Ground Thermal Regime by Data Assimilation of Sentinel-2-retrieved Fractional Snow-Covered Area.

IGARSS 2024

A. Bartsch, R. Tanguy, H. Bergstedt, X. Muri, Similarities in northern hemisphere permafrost ground temperature and sea ice extent change from 1997 to 2019.

5.6 Specific tasks

Session chairing

Strozzi, T: Space-borne studies of permafrost in the Arctic , 2024 European Polar Science Week, 3–6 September 2024, Copenhagen, Denmark.

Helena Bergstedt, In-Won Kim, Martijn Pallandt, Louise Farquharson, David Wårlind, Annett Bartsch, Rebecca Scholten: Permafrost dynamics, interactions, feedbacks, disturbances and GHG's across scales: perspectives from observation to modelling. EGU General Assembly 2024, 14–19 April 2024, Vienna, Austria,

Garten-Roer, I., Kelkar, K., Brardinoni, F. (conveners). Open session on Rock glaciers. 12th International Conference on Permafrost (ICOP), 16–20 June 2024, Whitehorse, Canada.

Pellet, C., Vivero, S., Cusicanqui, D., Hartl, L. Kellerer-Priklbauer, A. (conveners). New insights into the dynamics of rock glaciers. EGU General Assembly 2024, 14–19 April 2024, Vienna, Austria,

Pellet, C., Rouyet, L., Hu, Y. (conveners). Open session on Rock glaciers. 6th European Conference on Permafrost (EUCOP), 18–22 June 2023, Puigcerdà, Spain.

Projects in synergy with the Permafrost_cci rock glacier component

Full-scale rock glacier inventory of Switzerland in ongoing, through the work package 1 of the **RoDynAlpS** project "Rock glacier dynamics at multiple spatio-temporal scales in Switzerland" (2023–2027), funded by the Swiss National Foundation (SNF). The ongoing work is using the GIS tools and approaches developed in the framework of RGIK and Permafrost_cci.

The development of the database to store and disseminate RoGI and RGV products in supported by the **ORoDaPT** project "Open Rock Glacier Data Production Tools" (2024), funded SwissUniversities. ORoDaPT aims to develop tools to collect, process and analyse RoGI and RGV data, and design and implement a data management system. The project contributes to provide sustainable solutions for the dissemination and user exploitation of Permafrost_cci products.

RoGI and RGV product generation in the Italian Alps is supported by the **PARACELSO** project "Predictive Analysis, monitoRing, and mAnagement of Climate change Effects Leveraging Satellite Observations" (2024–2026), funded by the Italian Space Agency. WP4 deals with rock glaciers in Valle d'Aosta region (Western Italian Alps). Task 4.1: Region-wide InSAR-based kinematic characterization of rock glaciers (S1, CSK and SAOCOM). Task 4.2: InSAR-based RGV time series for a selected cluster of rock glaciers that may pose risk to infrastructure.

5.7 Student teaching and courses

MSc thesis from Lea Schmid (February 2024) "InSAR multi-annual velocity products on selected rock glaciers in the Swiss Alps", University of Fribourg (UNIFR), Switzerland. Supervisors: Prof. Reynald Delaloye, Dr. Line Rouyet.

BSc practical course in Geomorphology (spring semester 2023), University of Fribourg (UNIFR), Switzerland. Teachers: Prof. Reynald Delaloye and Dr. Thomas Echelard. Project conducted with students on testing the RoGI GIS tools and approaches developed in the framework of RGIK and Permafrost_cci in selected areas over the Swiss Alps.

Graduate GIS course (autumn semester 2023), University of Bologna (UniBo). Teacher: Ass.Prof. Francesco Brardinoni. Practical component on applying RoGI guidelines developed in the framework of RGIK and Permafrost_cci focusing on study areas in the Italian Alps.

One-day lecture and practical exercise on Remote Sensing of Permafrost Regions, as part of the MSc/PhD AG-330/830 course on Permafrost and Periglacial Environments (spring semester 2024), University Centre in Svalbard (UNIS). Teacher: Dr. Line Rouyet. Theory and use of InSAR in Svalbard, incl. applications on rock glaciers, as developed in Permafrost_cci.

Remote Sensing of Permafrost Regions, MSc Module taught by G. Grosse & I. Nitze at University of Potsdam (4 hrs/week; SS 2019, WS 2019/2020, WS 2020/2021, WS 2021/2022, WS 2022/23, WS 2023/24)

HEIBRiDS Seminar Series. I.Nitze: Machine-learning for mapping permafrost landscape dynamics. https://www.heibrids.berlin/

Potsdam Summer School 2021. I.Nitze: Wetting vs. Drying of Arctic Permafrost landscapes. https://potsdam-summer-school.org/

6 References

6.1 Bibliography

Bartsch, A., Höfler, A., Kroisleitner, C., Trofaier, A.M. (2016). Land Cover Mapping in Northern High Latitude Permafrost Regions with Satellite Data: Achievements and Remaining Challenges. Remote Sens., 8, 979.

Bartsch A., Ley S., Nitze I, Pointner G. and Vieira G. (2020). Feasibility Study for the Application of Synthetic Aperture Radar for Coastal Erosion Rate Quantification Across the Arctic. Front. Environ. Sci. 8:143. https://10.3389/fenvs.2020.00143

Biskaborn, B.K., Lanckman, J.-P., Lantuit, H., Elger, K., Streletskiy, D.A., Cable, W.L. and Romanovsky, V.E. (2015). The new database of the Global Terrestrial Network for Permafrost (GTN-P). Earth System Science Data, 7(2), 245–259. https://doi.org/10.5194/essd-7-245-2015

Biskaborn, B.K., Smith, S.L., Noetzli, J., Matthes, H., Vieira, G., Streletskiy, D.A., Schoeneich, P., Romanovsky, V.E., Lewkowicz, A.G., Abramov, A. and Allard, M. (2019). Permafrost is warming at a global scale. Nature Communications, 10(1), 264.

Bertone, A., Barboux, C., Bodin, X., Bolch, T., Brardinoni, F., Caduff, R., Christiansen, H. H., Darrow, M., Delaloye, R., Etzelmüller, B., Humlum, O., Lambiel, C., Lilleøren, K. S., Mair, V., Pellegrinon, G., Rouyet, L., Ruiz, L., and Strozzi, T. 2022. Incorporating InSAR kinematics into rock glacier inventories: insights from 11 regions worldwide, The Cryosphere, 16, 2769–2792. https://doi.org/10.5194/tc-16-2769-2022.

Brown R.J.E. (1970) Permafrost in Canada: Its influence on northern development. University of Toronto Press, Toronto 234 p.

Cable, W.L., Romanovsky, V.E. and Jorgenson, M.T. (2016). Scaling-up permafrost thermal measurements in western Alaska using an ecotype approach. Cryosphere, 10, 2517–2532.

Chadburn, S., Burke, E., Cox, P., Friedlingstein, P., Hugelius, G. and Westermann, S. (2017a). An observation-based constraint on permafrost loss as a function of global warming, Nature Climate Change, doi:10.1038/nclimate3262.

Chadburn, S.E., Krinner, G., Porada, P., Bartsch, A., Beer, C., Belelli Marchesini, L., Boike, J., Ekici, A., Elberling, B., Friborg, T., Hugelius, G., Johansson, M., Kuhry, P., Kutzbach, L., Langer, M., Lund, M., Parmentier, F.-J.W., Peng, S., Van Huissteden, K., Wang, T., Westermann, S., Zhu, D., and Burke, E.J. (2017b). Carbon stocks and fluxes in the high latitudes: using site-level data to evaluate Earth system models, Biogeosciences, 14, 5143-5169. https://doi.org/10.5194/bg-14-5143-2017.

Christensen, O.B., Drews, M., Christensen, J.H., Dethloff, K., Ketelsen, K., Hebestadt, I. and Rinke, A. (2007), The HIRHAM regional climate model, version 5, Tech. Rep. 06-17, Dan. Meteorol. Inst., Copenhagen, http://www.dmi.dk/dmi/tr06-17.pdf.

Dutch, V. R., Rutter, N., Wake, L., Sandells, M., Derksen, C., Walker, B., ... & Boike, J. (2022). Impact of measured and simulated tundra snowpack properties on heat transfer. *The Cryosphere*, *16*(10), 4201-4222.

Gisnås, K., Westermann, S., Schuler, T.V., Litherland, T., Isaksen, K., Boike, J., and Etzelmüller, B. (2014). A statistical approach to represent small-scale variability of permafrost temperatures due to snow cover. The Cryosphere, 8, 2063-2074. https://doi.org/10.5194/tc-8-2063-2014

Grosse G., Robinson J.E., Bryant R., Taylor M.D., Harper W., DeMasi A., Kyker-Snowman E., Veremeeva A., Schirrmeister L. and Harden J. (2013). Distribution of late Pleistocene ice-rich syngenetic permafrost of the Yedoma Suite in east and central Siberia, Russia. U.S. Geological Survey Open File Report 2013-1078, 37p.

Heginbottom, J.A. (1984). The mapping of permafrost. Canadian Geographer, Vol. 28, No.1, pp. 78-83.

Heginbottom, J.A., Radburn, L.K. (1992). Permafrost and Ground Ice Conditions of Northwestern Canada (Mackenzie Region). National Snow and Ice Data Center, Boulder, CO, USA.

IPCC (2013). Climate Change 2013: The Physical Science Basis. Contribution of Working Group I to the Fifth Assessment Report of the Intergovernmental Panel on Climate Change [Stocker, T.F., D. Qin, G.-K. Plattner, M. Tignor, S.K. Allen, J. Boschung, A. Nauels, Y. Xia, V. Bex and P.M. Midgley (eds.)]. Cambridge University Press, Cambridge, United Kingdom and New York, NY, USA, 1535 pp.

IPCC (2019). IPCC Special Report on the Ocean and Cryosphere in a Changing Climate (SROCC).

IPCC (2021). Climate Change 2021: The Physical Science Basis. Contribution of Working Group I to the Sixth Assessment Report of the Intergovernmental Panel on Climate Change [Masson-Delmotte, V., P. Zhai, A. Pirani, S.L. Connors, C. Péan, S. Berger, N. Caud, Y. Chen, L. Goldfarb, M.I. Gomis, M. Huang, K. Leitzell, E. Lonnoy, J.B.R. Matthews, T.K. Maycock, T. Waterfield, O. Yelekçi, R. Yu, and B. Zhou (eds.)]. Cambridge University Press.

Jones, B.M., Kolden, C.A., Jandt, R., Abatzoglou, J.T., Urban, F., & Arp, C.D. (2009). Fire Behavior, Weather, and Burn Severity of the 2007 Anaktuvuk River Tundra Fire, North Slope, Alaska. Arctic, Antarctic, and Alpine Research, 41(3), 309–316. https://doi.org/10.1657/1938-4246-41.3.309

Kellerer-Pirklbauer-Eulenstein, A., Bodin, X., Delaloye, R., Lambiel, C., Gärtner-Roer, I., Bonnefoy-Demongeot, M., ... & Zumiani, M. (2024). Acceleration and interannual variability of creep rates in mountain permafrost landforms (rock glacier velocities) in the European Alps in 1995–2022. Environmental Research Letters. https://doi.org/10.1088/1748-9326/ad25a4.

Kelley, A.M., Epstein, H.E., and Walker, D.A. (2004). Role of vegetation and climate in permafrost active layer depth in arctic tundra of northern Alaska and Canada, J. Glaciol. Climatol., 26, 269–273.

Koven, C.D., W.J. Riley, and Stern, A. (2013). Analysis of Permafrost Thermal Dynamics and Response to Climate Change in the CMIP5 Earth System Models. J. Climate, 26, 1877–1900

Kudryavtsev V.A., (Editor) (1978). Obshcheye merzlotovedeniya (Geokriologiya) (General permafrost science) In Russian. Izd. 2, (Edu 2) Moskva (Moscow), Izdatel'stvo Moskovskogo Universiteta, (Moscow University Editions), 404 pp

Lawrence, D. M., Fisher, R. A., Koven, C. D., Oleson, K. W., Swenson, S. C., Bonan, G., ... & Zeng, X. (2019). The Community Land Model version 5: Description of new features, benchmarking, and impact of forcing uncertainty. *Journal of Advances in Modeling Earth Systems*, *11*(12), 4245-4287.

Matthes, H., Rinke, A. and Dethloff (2015). K.,Recent changes in Arctic temperature extremes: warm and cold spells during winter and summer, Environmental Research Letters, 10(11).

Matthes, H., Rinke, A., Zhou, X., and Dethloff, K. (2017). Modelling atmosphere and permafrost in the Arctic using a new regional coupled atmosphere-land model, Journal of Geophysical Research Atmospheres, 122, 7755–7771.

McGuire A.D., Koven C., Lawrence D.M., Clein J.S., Xia J., Beer C., Burke E., Chen G., Chen X., Delire C., Jafarov E., MacDougall A.H., Marchenko S., Nicolsky D., Peng S., Rinke A., Saito K., Zhang W., Alkama R., Bohn T.J., Ciais P., Decharme B., Ekici A., Gouttevin I., Hajima T., Hayes D.J., Ji D., Krinner G., Lettenmaier D.P., Luo Y., Miller P.A., Moore J.C., Romanovsky V., Schädel C., Schaefer K., Schuur E.A.G., Smith B., Sueyoshi T. snf Zhuang Q. (2016:).Variability in the sensitivity among model simulations of permafrost and carbon dynamics in the permafrost region between 1960 and 2009, 2016: Global Biogeochemical Cycles. https://doi:10.1002/2016GB005405

Muller S.W. (1943). Permafrost or permanently frozen ground and related engineering problems. U.S. Engineers Office, Strategic Engineering Study, Special Report No. 62. 136p. (Reprinted in 1947, J. W. Edwards, Ann Arbor, Michigan, 231p.)

Nelson, F.E., Shiklomanov, N.I., Mueller, G.R., Hinkel, K.M., Walker, D.A., and Bockheim, J.G. (1997). Estimating Active-Layer Thickness over a Large Region: Kuparuk River Basin, Alaska, USA, Arctic Alpine Res., 29, 4, https://doi:10.2307/1551985.

Nitze, I., Grosse, G., Jones, B.M., Arp, C.D., Ulrich, M., Fedorov, A., and Veremeeva, A. (2017). Landsat-based trend analysis of lake dynamics across northern permafrost regions. Remote Sensing, 9(7), 640.

Nitze, I., Grosse, G., Jones, B.M., Romanovsky, V.E. and Boike, J. (2018a). Remote sensing quantifies widespread abundance of permafrost region disturbances across the Arctic and Subarctic. Nature communications, 9(1), 1-11.

Nitze, I., Grosse, G., Jones, B.M., Romanovsky, V.E and Boike, J. (2018b). Data Documentation v1. 0: Remote sensing quantifies widespread abundance of permafrost region disturbances across the Arctic and Subarctic.

Nitze, I., Cooley, S., Duguay, C., Jones, B. M. and Grosse, G. (2020). The catastrophic thermokarst lake drainage events of 2018 in northwestern Alaska: Fast-forward into the future. The Cryosphere Discussions, 1-33.

Obu, J., Westermann, S., Kääb, A. and Bartsch, A. (2018). Ground Temperature Map, 2000-2016, Northern Hemisphere Permafrost (p. 40 data points) [Text/tab-separated-values]. PANGAEA - Data Publisher for Earth & Environmental Science. https://doi.org/10.1594/PANGAEA.888600

Obu, J., Westermann, S., Bartsch, A., Berdnikov, N., Christiansen, H.H., Dashtseren, A., Delaloye, R., Elberling, B., Etzelmüller, B., Kholodov, A. and Khomutov, A. (2019). Northern Hemisphere permafrost map based on TTOP modelling for 2000–2016 at 1 km2 scale. Earth-Science Reviews.

Obu, J. (2021). How Much of the Earth's Surface is Underlain by Permafrost? Journal of Geophysical Research: Earth Surface, 126(5). https://doi.org/10.1029/2021JF006123

Olefeldt, D., Goswami, S., Grosse, G., Hayes, D., Hugelius, G., Kuhry, P., McGuire, A. D., Romanovsky, V. E., Sannel, A. B. K., Schuur, E. A. G., & Turetsky, M. R. (2016). Circumpolar distribution and carbon storage of thermokarst landscapes. Nature Communications, 7(1), 13043. https://doi.org/10.1038/ncomms13043

Pellet, C., Bodin, X., Cusicanqui, D., Delaloye, R., Kaufmann, V., Noetzli, J., Thibert, E., Vivero, S., & Kellerer-Pirklbauer, A. 2023. Rock glacier velocity. In State of Climate 2022 (Vol. 104, pp. 41–42). https://doi.org/10.1175/2023BAMSStateoftheClimate.1.

PERMOS 2023. Swiss Permafrost Bulletin 2022. Noetzli, J. and Pellet, C. (eds.) 22 pp. https://doi.org/10.13093/permos-bull-2023.

Romanovsky, V.E., Smith, S.L., and Christiansen, H.H. (2010). Permafrost thermal state in the polar Northern Hemisphere during the international polar year 2007–2009: A synthesis. Permafrost and Periglacial Processes, 21(2), 106–116.

Schaefer, K., Lantuit, H., Romanovsky, V.E., Schuur, E.A.G. and Witt, R. (2014). The impact of the permafrost carbon feedback on global climate. Environmental Research Letters, 9, 085003.

Strauss J., Schirrmeister L., Grosse G., Fortier D., Hugelius G., Knoblauch C., Romanovsky V.E., Schädel C., Schneider von Deimling T., Schuur E.A.G., Shmelev D., Ulrich M. snf Veremeeva A.. (2017): Deep Yedoma permafrost: A synthesis of depositional characteristics and carbon vulnerability. Earth-Science Reviews, 172: 75-86. https://doi: 10.1016/j.earscirev.2017.07.007

Schuur E.A., McGuire A.D., Schädel C., Grosse G., Harden J.W., Hayes D.J., Hugelius G., Koven C.D., Kuhry P., Lawrence D.M. and Natali S.M. (2015) Climate change and the permafrost carbon feedback. Nature. Apr;520(7546):171.

Slater, A.G. and D.M. Lawrence (2013). Diagnosing Present and Future Permafrost from Climate Models. J. Climate, 26, 5608–5623, https://doi.org/10.1175/JCLI-D-12-00341.1

Strauss J., Schirrmeister L., Grosse G., Fortier D., Hugelius G., Knoblauch C., Romanovsky V.E., Schädel C., Schneider von Deimling T., Schuur E.A.G., Shmelev D., Ulrich M. and Veremeeva A.. (2017). Deep Yedoma permafrost: A synthesis of depositional characteristics and carbon vulnerability. Earth-Science Reviews, 172: 75-86. doi: 10.1016/j.earscirev.2017.07.007

Turetsky, M.R., Abbott, B.W., Jones, M.C., Walter Anthony, K., Olefeldt, D., Schuur, E.A.G., Koven, C., McGuire, A.D., Grosse, G., Kuhry, P., Hugelius, G., Lawrence, D.M., Gibson, C., and Sannel, A.B.K. (2019). Permafrost collapse is accelerating carbon release. Nature, 569(7754), 32–34. https://doi.org/10.1038/d41586-019-01313-4

Vincent, W.F., Lemay, M. and Allard, M. (2017). Arctic permafrost landscapes in transition: towards an integrated Earth system approach. Arctic Science, 3(2), 39-64.

Westermann, S., Østby, T., Gisnås, K., Schuler.T. and Etzelmüller, B. (2015) A ground temperature map of the North Atlantic permafrost region based on remote sensing and reanalysis data, The Cryosphere, 9, 1303-1319, https://doi:10.5194/tc-9-1303-2015.

Williams, J.R. (1965). Groundwater in permafrost regions: An annotated bibliography. U.S. Geological Survey, Professional Paper 696, 83p.

Windirsch, T., Grosse, G., Ulrich, M., Schirrmeister, L., Fedorov, A. N., Konstantinov, P. Y., Fuchs, M., Jongejans, L. L., Wolter, J., Opel, T., and Strauss, J. (2020). Organic carbon characteristics in ice-rich permafrost in alas and Yedoma deposits, central Yakutia, Siberia, Biogeosciences, 17, 3797–3814, https://doi.org/10.5194/bg-17-3797-2020

van Everdingen R.O. (1985). Unfrozen permafrost and other taliks. Workshop on Permafrost Geophysics, Golden, Colorado, October 1984 (J. Brown, M.C. Metz, P. Hoekstra, Editors). U.S. Army, C.R.R.E.L., Hanover, New Hampshire, Special Report 85-5, pp.101-105

Yamazaki, D., Ikeshima, D., Tawatari, R., Yamaguchi, T., O'Loughlin, F., Neal, J. C., Sampson, C. C., Kanae, S., & Bates, P. D. (2017). A high-accuracy map of global terrain elevations: Accurate Global Terrain Elevation map. Geophysical Research Letters, 44(11), 5844–5853. https://doi.org/10.1002/2017GL072874

6.2 Acronyms

ACOP	Asian Conference on Permafrost
ALT	Active Layer Thickness
Arctic CORDEX	Coordinated Regional Climate Downscaling Experiment
ASSW	Arctic Science Summit Week
AWI	Alfred Wegener Institute Helmholtz Centre for Polar and Marine Research
B.GEOS	b.geos GmbH
CALM	Circumpolar Active Layer Monitoring
CliC	Climate and Cryosphere project
CLM4	Land Community Model Version 4
CLM5	Land Community Model Version 5
CCI	Climate Change Initiative

CMIP-6 The Coupled Model Intercomparison Project
CMUG Climate Modelling User Group
CRESCENDO Coordinated Research in Earth Systems and Climate: Experiments, Knowledge, Dissemination and Outreach
CRG Climate Research Group
ECV Essential Climate Variable
EO Earth Observation
ESA European Space Agency
ESA DUE ESA Data User Element
FT2T Freeze-Thaw to Temperature
GAMMA Gamma Remote Sensing AG
GCOS Global Climate Observing System
GCW Global Cryosphere Watch
GTD Ground Temperature at certain depth
GT Ground Temperature
GTN-P Global Terrestrial Network for Permafrost
GTOS Global Terrestrial Observing System
GUIO Department of Geosciences University of Oslo
HIRHAM High Resolution Limited Area Model
HRPC Hot Spot Regions of Permafrost Change
IASC International Arctic Science Committee
ILAMB International Land Model Benchmarking
IPA International Permafrost Association
IPCC Intergovernmental Panel on Climate Change
LS3MIP Land Surface, Snow and Soil Moisture
MAGT Mean Annual Ground Temperature
NetCDF Network Common Data Format
NSIDC National Snow and Ice Data Center
PCN Permafrost Carbon Network
PE Permafrost Extent
PERMOS Swiss Permafrost Monitoring Network
PF Permafrost
PFR Permafrost Fraction
PSTG Polar Space Task Group
PUG Product User Guide
PVIR Product Validation and Intercomparison Report
RASM Regional Arctic System Model
RCOP Regional Conference on Permafrost
RD Reference Document
RMSE Root Mean Square Error
RS Remote Sensing
SAR Synthetic Aperture Radar
SCAR Scientific Committee on Antarctic Research
SU Department of Physical Geography Stockholm University

TSP	Thermal State of Permafrost
UNIFR	Department of Geosciences University of Fribourg
URD	Users Requirement Document
WCRP	World Climate Research Program
WMO	World Meteorological Organisation
WMO OSCAR	Observing Systems Capability Analysis and Review Tool
WUT	West University of Timisoara